Rm101 c.1

UNIVERSITY OF WASHINGTON
DEPARTMENT OF
OCEANOGRAPHY

TECHNICAL REPORT NO. 98

DISTRIBUTION OF BEACH SEDIMENT NEAR THE COLUMBIA RIVER

by

Ronald L. Ballard

U.S. Atomic Energy Commission
Contract AT(45-1)-1725
and
Office of Naval Research
Contract Nonr-477(10)
Project 083-012

Reference M64-16
February 1964

DEPARTMENT OF OCEANOGRAPHY
UNIVERSITY OF WASHINGTON
SEATTLE 5, WASHINGTON 98105

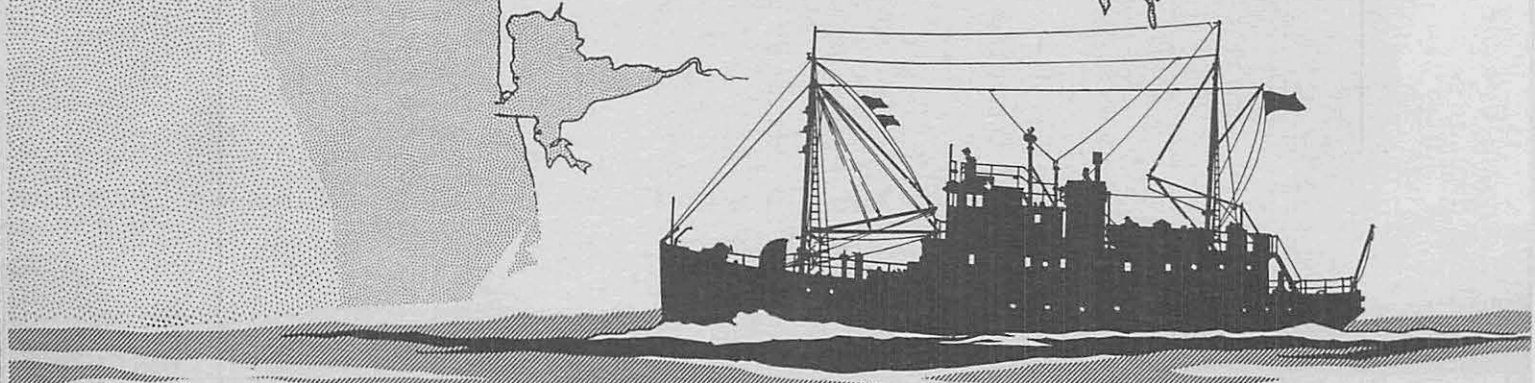

SEATTLE, WASHINGTON 98105

UNIVERSITY OF WASHINGTON
DEPARTMENT OF OCEANOGRAPHY
Seattle 5, Washington

TECHNICAL REPORT NO. 98

DISTRIBUTION OF BEACH SEDIMENT NEAR THE COLUMBIA RIVER

by

Ronald L. Ballard

U. S. Atomic Energy Commission
Contract AT(45-1)-1725
and
Office of Naval Research
Contract Nonr-477(10)
Project 083-012

Reference M64-16
February 1964

Clifford A. Barnes

CLIFFORD A. BARNES
Principal Investigator

R. H. Fleming

RICHARD H. FLEMING
Executive Officer

Reproduction in whole or in part is permitted
for any purpose of the United States Government

DISTRIBUTION OF BEACH SEDIMENT NEAR THE COLUMBIA RIVER

ABSTRACT

The coastline near the Columbia River, between Tillamook Head, Oregon and Grays Harbor, Washington, is characterized by prograding beaches in contrast to the rest of the Washington-Oregon coast where actively eroding sea cliffs are present. The Columbia River appears to be the major contributor of sediment to the beaches and probably accounts for their prograding character. Littoral transport of material from coastal erosion probably has some effect on the sediment budget, but coastal barriers of promontories and estuaries limit influx of this material. Some material is added to the beach as a result of jetty breakdown, especially near Grays Harbor, Washington. Willapa Bay apparently contributes only minor amounts of sediment to the area.

The net direction of beach sediment movement near the Columbia River appears to be northward. Seasonal changes in the direction of wave attack complicate the analysis, but the greater energy associated with winter wave conditions is directed northward and probably results in a predominant northerly sediment movement. Mechanical and heavy mineral analyses are consistent with the results of wave studies.

ACKNOWLEDGMENTS

The author is indebted to the following members of the Department of Oceanography for their assistance in the preparation of this report: Drs. Joe S. Creager, M. Grant Gross, Clifford A. Barnes, T. Saunders English, Mrs. Monique Rona, Mr. Don Doyle, Mr. James Woodruff, and Miss Tomilynn Willits.

This work was supported by the United States Atomic Energy Commission, Contract AT(45-1)-1725 and the Office of Naval Research, Contract Nonr-477(10), Project 083-012.

TABLE OF CONTENTS

INTRODUCTION 1
Objectives 1
Previous Work 1
Description of the Area 8
Regional Geology 10
Climate 11
Oceanographic Conditions 12
FIELD WORK 15
ANALYTICAL METHODS AND PRESENTATION OF DATA 17
Texture and Composition of Sediments 17
Mean Grain-Size 17
Sorting 25
Skewness 30
Heavy Minerals 30
Waves 36
Steepness 36
Energy 42
DISCUSSION AND INTERPRETATION 51
Source of Sediments 51
Direction of Sediment Movement 56
PROPOSED ANNUAL SEQUENCE OF EVENTS 66
CONCLUSIONS 67
REFERENCES 69

Table of Contents (continued)

APPENDIX I 76

APPENDIX II 80

APPENDIX III 81

LIST OF TABLES

I. Sample locations and size statistics according to Inman (1952). . . . 18

II. Averaged mean grain-size values (M_ϕ) for the various beach zones 26

III. Sorting values (σ_ϕ) for the various beach zones 29

IV. Skewness values (α_ϕ) for the various beach zones 32

V. Relative frequencies of heavy and magnetic minerals for the study area 34

VI. Relative percent of selected heavy minerals at various stations 37

VII. Relative frequency of waves with given steepness (H_o/L_o) values from various directions 41

VIII. Longshore component of wave energy flux for a point south (S) and a point north (N) of the Columbia River as a result of seas and swells from the given directions 45

LIST OF FIGURES

1. Pacific Border Province 2

2. Changes in Clatsop Beach, Oregon from 1870 to 1961 4

3. Relationship of volcanic rocks to associated drainage patterns of the Pacific Northwest 5

4. Depth changes near the mouth of the Columbia River for a period from 1877 to 1926 6

5. Depth changes near the mouth of the Columbia River for a period from 1926 to 1958 7

6. Study area showing beach zones and sampling stations 9

7. Typical beach cross-section showing sample locations and beach nomenclature 16

8. Graph of seasonal variation of mean grain size (Mϕ) 24

9. Seasonal variations of mean grain size for the trough, 20-foot, and 30-foot samples 27

10. Seasonal variations in sorting coefficients ($\sigma\phi$) along the beach for the trough, 20-foot, and 30-foot samples 28

11. Seasonal variations in skewness values ($\alpha\phi$) along the beach for the trough, 20-foot, and 30-foot samples. 31

12. Variations of heavy and magnetic minerals compared along the beach 33

13. Heavy and magnetic mineral variations for summer samples, averaged values 35

14. The composition of a selected suite of heavy minerals as a function of distance along the beach 38

15. Ratios of (Hypersthene/Hornblende) and (other Amphiboles/ Hornblende) compared 39

16. Relative frequency and direction of deep-water waves with steepness values of H_o/L_o = 0.015 to 0.025 43

17. Relative magnitude and direction of longshore energy flux south of the Columbia River 47

List of Figures (continued)

18. Relative magnitude and direction of longshore energy flux north of the Columbia River 48

19. Energy diagram representing average annual longshore component of wave energy flux in ft.lbs./foot of beach 50

INTRODUCTION

Objectives

The objectives of this report are to describe the sediments of the ocean beaches in the vicinity of the Columbia River and to determine the relationships among the regional topography, the processes active in the beach zone, and the properties of the sediments.

The beaches from Tillamook Head, Oregon to Grays Harbor, Washington are the result of the interaction of several groups of complex factors:

1. The geologic province.
2. The forces that modify the beach, associated with a regime that includes wind, waves, and currents.
3. The physical and mineralogical composition of the sedimentary material that makes up the beach.

The area was studied using this frame of reference as a guide. The geologic province that includes the study area was described, including some description of the mineralogy and drainage. Wind and wave data were studied so that their relative effects on the beaches could be determined. The sediments that form the beach area were described in terms of selected mechanical, chemical, and mineralogical parameters. These data were used in an attempt to determine the primary mode of formation of the beach and the net direction of sediment movement.

Previous Work

The geology of portions of the Pacific Border Province (Figure 1) has been described by several workers (Hodge, 1938; Lowry and Baldwin, 1952; Baldwin, 1959). Coastal regions of the Olympic Peninsula have been studied by Arnold (1906) and Lupton (1915). The geology of Oregon was discussed by

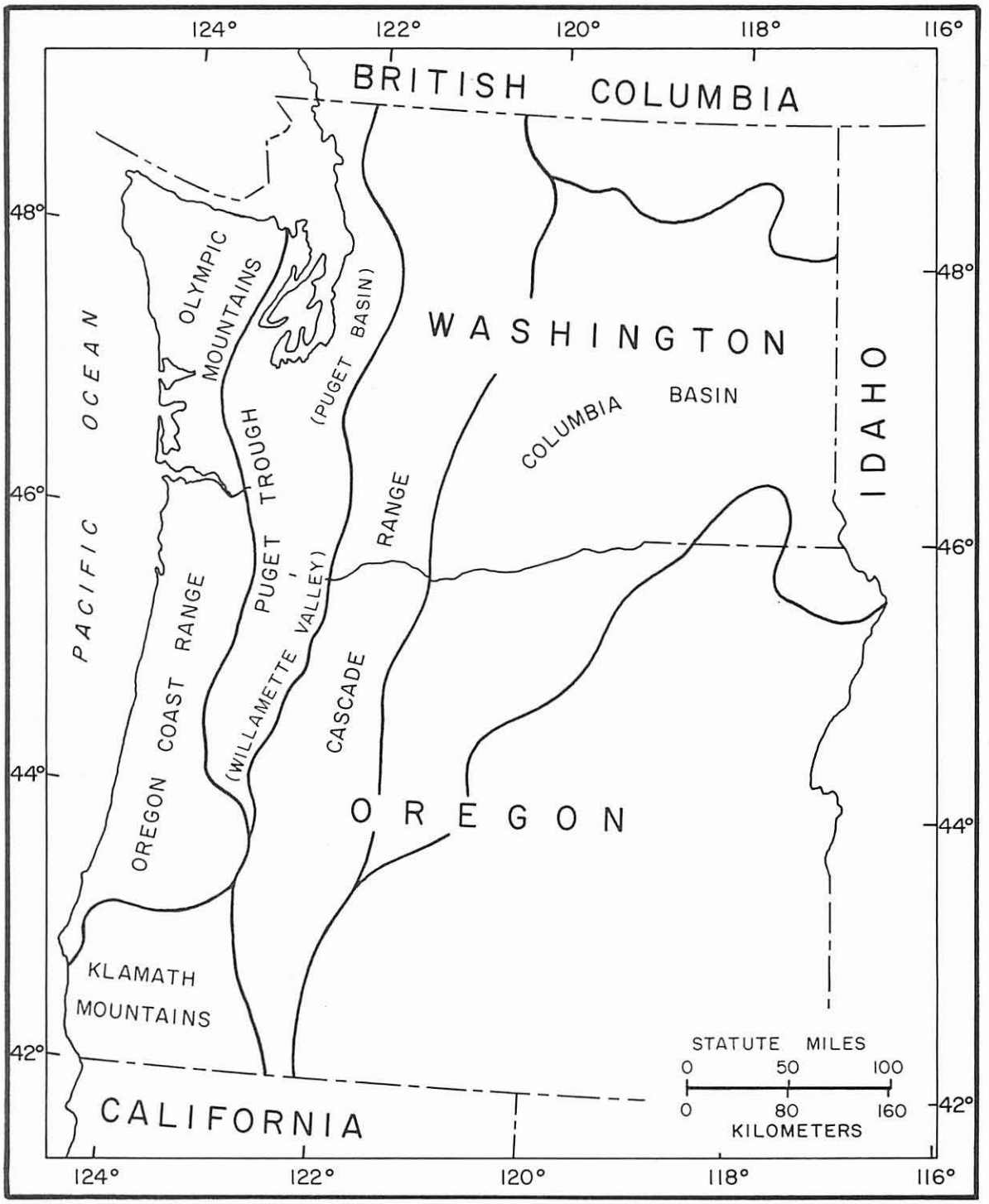

Fig. 1: Pacific Border Province (after Dicken, 1961 in part).

Baldwin (1959), and Dicken (1961) described some recent changes in the morphology of the Oregon coast (Figure 2). The basaltic rocks of the Pacific Border Province have been studied and differentiated by means of their characteristic mineral suites (Waters, 1962) (Figure 3).

Several workers have studied local heavy mineral concentrations in beach deposits along the Washington-Oregon coast (Honar, 1918; Pardee, 1929, 1934; Twenhofel, 1943; Griggs, 1945; Hundhausen, 1947). Twenhofel (1946a,b) also described the physical and mineral composition of the beach sands along the Oregon coast. Some work has been done on coastal sand dunes of Oregon and Washington by McLaughlin, Willard, and Brown (1942) and Cooper (1958, 1959).

Oceanic circulation in the vicinity of the Washington coast was studied by Barnes and Pacquette (1957) and Tully and Barber (1961). Considerable attention has also been given to phenomena affecting the mouth of the Columbia River (e.g., U.S. Army Corps of Engineers, 1933, 1938; U.S. Tidal Model Laboratory, 1935, 1936; O'Brien, 1948, 1951; Lockett, 1962), and Grays Harbor (U.S. Army Corps of Engineers, 1951). The Portland Office of the Corps of Engineers (personal communication) obtained data concerning changes of bathymetry in the vicinity of the Columbia River. These data were plotted as depth changes during the period from 1877 to 1926 (Figure 4) and from 1926 to 1958 (Figure 5). The first figure represents changes from immediately prior to construction of the south jetty (1885 to 1895) to a time following construction of the north jetty (1913 to 1917). The second figure represents subsequent changes.

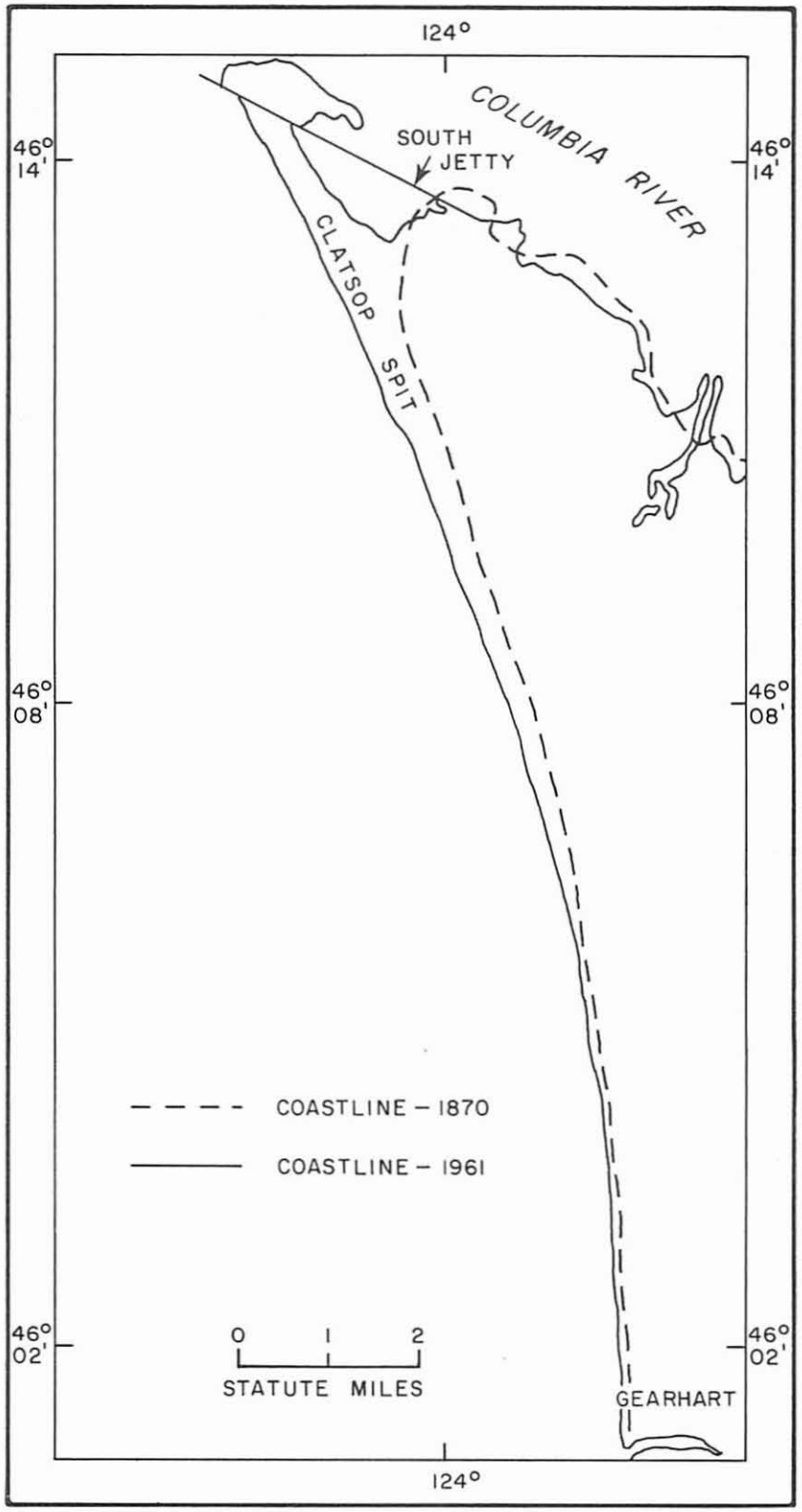

Fig. 2: Changes in Clatsop Beach, Oregon from 1870 to 1961. Based on U. S. C. and G. S. charts of 1874 and topographic sheets of 1961 (from Dicken, 1961).

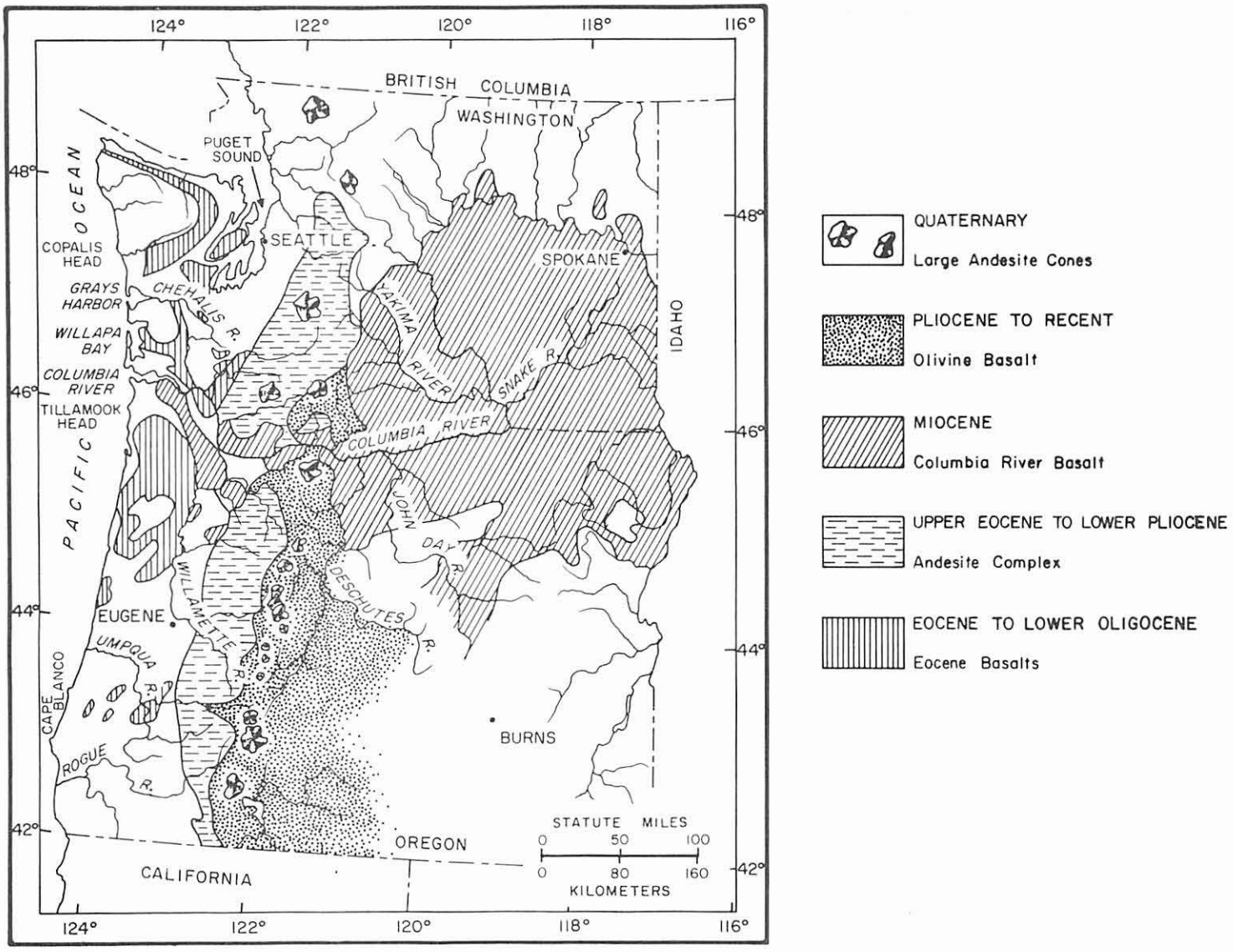

Fig. 3: Relationship of volcanic rocks to associated drainage patterns of the Pacific Northwest (modified from Waters, 1962).

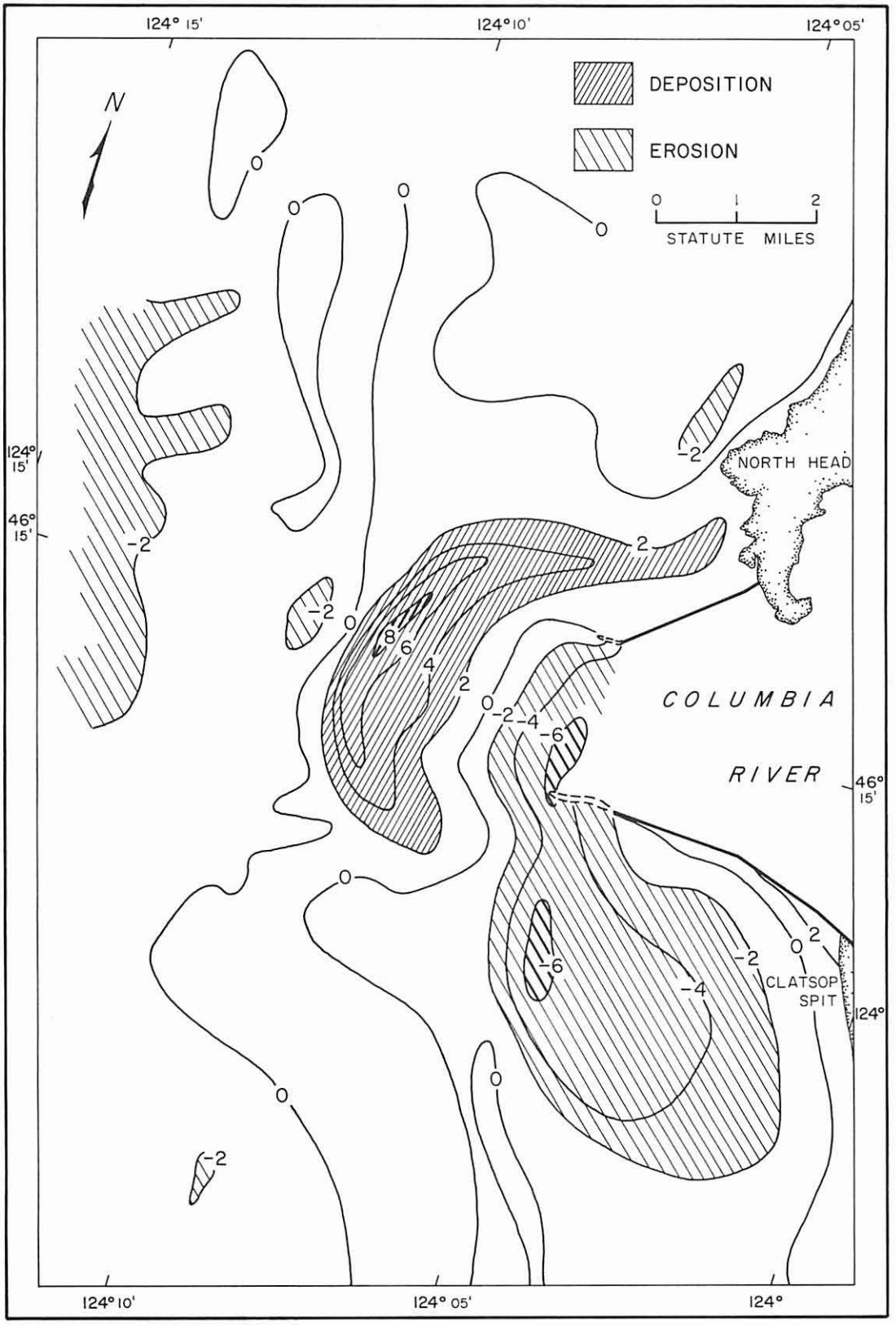

Fig. 4: Depth changes near the mouth of the Columbia River for a period from 1877 to 1926. Values are reported in fathoms and contoured at 2-fathom intervals. Modified from U. S. Army Corps of Engineers chart, Rivers and Harbors Section.

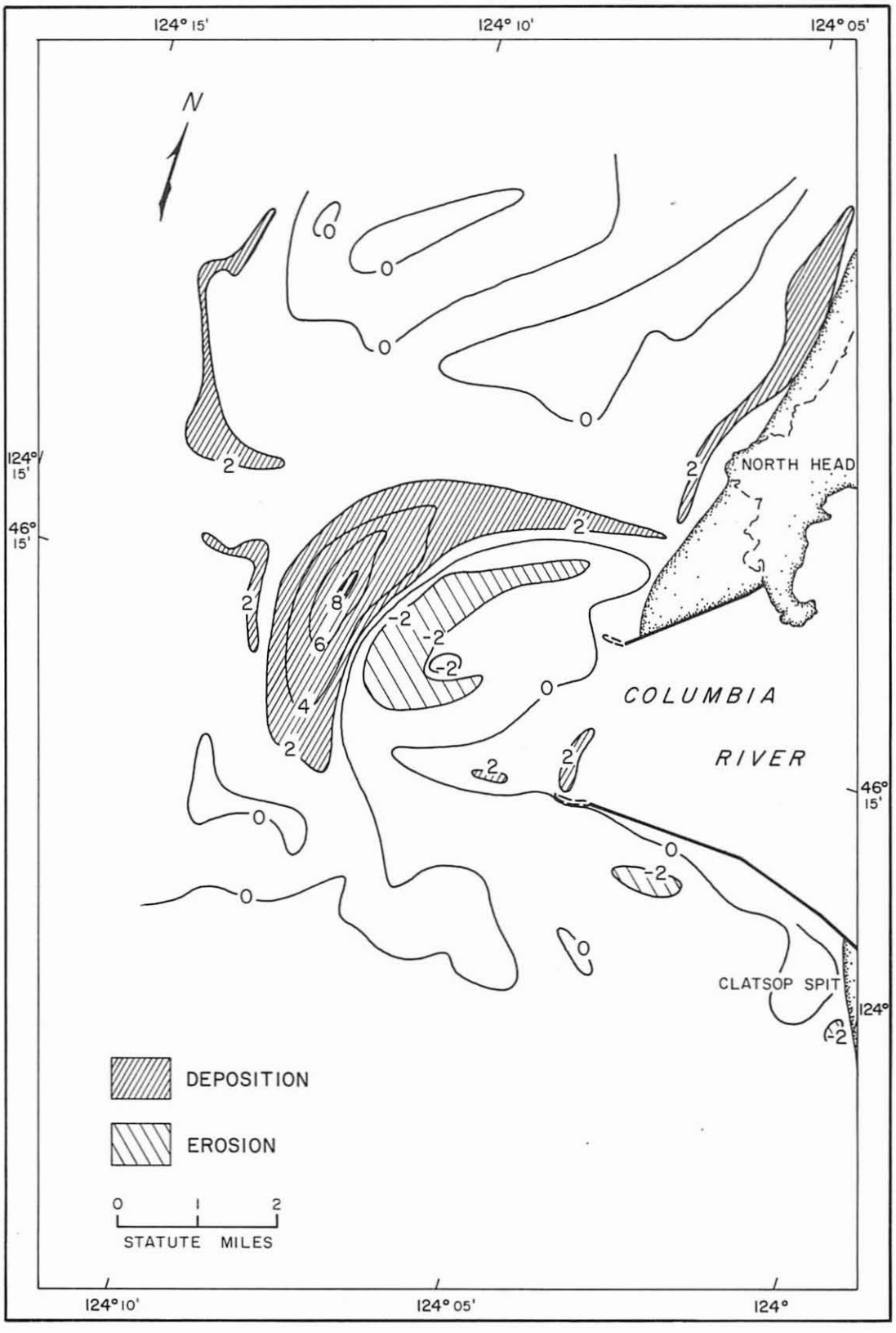

Fig. 5: Depth changes near the mouth of the Columbia River for a period from 1926 to 1958. Values are reported in fathoms and contoured at 2-fathom intervals. Modified from U. S. Army Corps of Engineers chart, Rivers and Harbors Section.

Description of the Area

The beach area involved in this study extends 70 miles[1] (112 kilometers) from Tillamook Head, Oregon to Grays Harbor, Washington (46°00' to 47°00'N Lat. and 127°00'W Long., Figure 6). Sand dunes and beach ridges are found along the entire beach and extend inland for an average distance of about 2 miles (3.2 kilometers). The dunes and ridges are oriented parallel to the shoreline, broken only by the estuary of the Columbia River, Willapa Bay entrance, and Grays Harbor entrance. The beach ridges are formed as a result of stabilization of sand dunes by vegetation (Cooper, 1958). They have an average height of 3 to 6 meters (9.8 to 19.6 feet) with variable widths. Usually 3 to 5 ridges are present.

Clatsop Beach extends from Tillamook Head, Oregon to the mouth of the Columbia River and from the present shoreline to an upland area about 6 kilometers (3.7 miles) inland. It is characterized by beach ridges resulting from vegetative stabilization of sand dunes. The zone is termed an attached foreland by Cooper (1958).

Long Beach is a peninsula extending northward from the Columbia River to Willapa Bay. It is composed of parallel beach ridges with many small, elongate dune lakes and bogs slightly above sea level. The southern half of the Long Beach peninsula is completely stabilized with ridges extending almost to the shore, while the northern half shows marked evidence of erosion, indicated by blow-outs and sand dunes invading the forested areas east of the shoreline. The northernmost 4 kilometers (2.5 miles) of the peninsula is almost devoid of vegetation. East of the ridges, on the

---

[1] Statute miles were used throughout because most of the distances were measured on land.

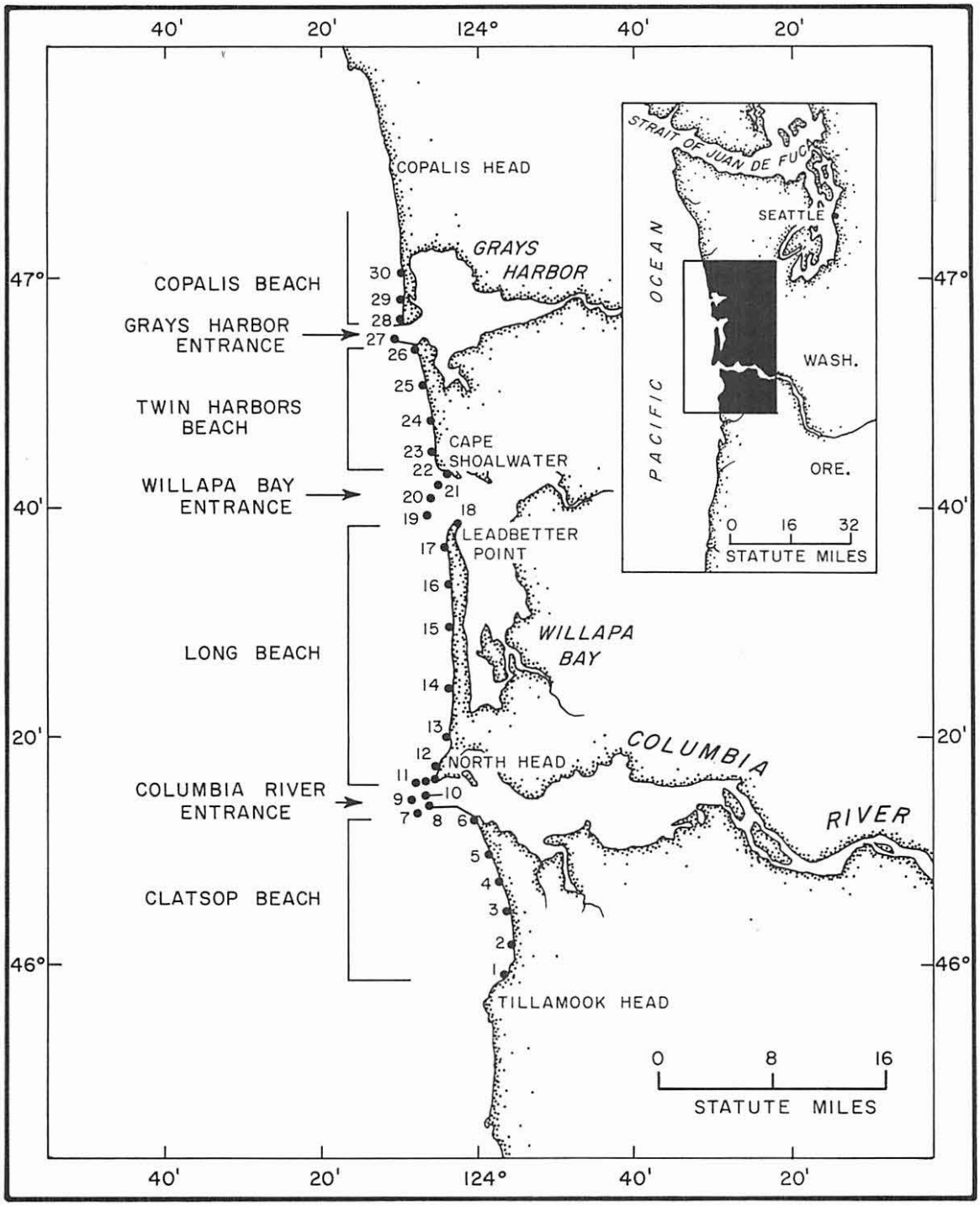

Fig. 6: Study area showing beach zones and sampling stations.

bayward side of the peninsula, a narrow strip of sand merges with the tidal flats of Willapa Bay. A triangular shaped sand deposit formed between North Head and the north jetty of the Columbia River after construction of the north jetty (1913-1917).

Twin Harbors Beach is located between Willapa Bay and Grays Harbor and is similar to Long Beach. The southern part consists of a foreland of beach ridges adjoining highlands immediately to the east. The northern portion is a peninsula extending to the Grays Harbor entrance. The entire zone consists of stabilized and forested beach ridges being invaded by an active sand dune.

Copalis Beach extends north from Grays Harbor and is similar to those to the south, with stabilized beach ridges parallel to the coast. It is attached at Copalis Head to the north. The peninsula formed by Copalis Beach is the only major beach feature of the Washington coastline that extends toward the south.

Regional Geology.-- The geologic province that includes the study area was termed the Pacific Border Province (Figure 1) by Fenneman (1931). This province is characterized by a series of structurally related north-south trending valleys, bounded to the east and west by mountain chains. The valleys form a synclinorium, called the Puget Trough (Fenneman, 1931), which contains the Puget Basin to the north, and the Willamette Valley to the south. The valleys are bounded on the east by the Cascade Mountains and on the west by the Coast Ranges. The Coast Ranges include the Olympic Mountains in Washington, the Oregon Coast Range of northern Oregon, and the Klamath Mountains of southern Oregon.

The Coast Ranges are characterized by cliffs which provide evidence

of an eroding coastline (Arnold, 1906; Campbell, 1962). Terraces are common along the coast, suggesting that the coastline has been rising in the recent geologic past (Dicken, 1961). However, the latest movement was probably one of subsidence, as shown by the drowned river valleys throughout the area (Dicken, 1961).

Although the valleys are structurally related, their topographic features suggest different geologic histories. The Puget Basin topography shows the effects of glaciation that terminated in a broad glacial outwash plain extending to the Pacific Ocean by way of the Chehalis River Valley (Fenneman, 1931; Glover, 1940). The Willamette River Valley is drained by the Willamette River, which carries a heavy sediment load derived from the surrounding mountains (Fenneman, 1931).

Climate.-- The study area is located approximately in the center of a zone of prevailing westerlies and the local winds vary predominantly from northwest to southwest throughout most of the year. This results in a climate controlled primarily by maritime influences. The average annual temperature at North Head, Washington (Figure 6), for a 63 year period, was 10.0°C with an annual range of about 8.6°C.

The general air circulation is controlled to a great extent by a permanent high pressure system off the coast. In the summer it is located at about 40°N and 150°W. A low pressure zone develops over the southwest United States (Strahler, 1960) and the complex interaction of these pressure zones causes a general air movement from west-to-northwest over the Washington-Oregon coast. During the winter, the high pressure zone shifts about 10° southward and a low pressure zone forms over the Aleutians, resulting in winds that arrive from the west-to-southwest along the Oregon-

Washington coast. Temperature gradients from land to sea cause minor fluctuations in the general pattern.

Coastal mountain barriers have a decided effect on the general wind regime, deflecting the winds to a direction following the trend of the mountains. However, the general topography in the immediate vicinity of the Columbia River is rather low and the deflecting effect is diminished so that normal oceanic wind conditions prevail (Cooper, 1958). This condition is reflected in the sand dunes in the vicinity of the Columbia River as compared to those in southern Oregon. The southern Oregon dunes are often irregular in shape as a result of variable wind directions while those in the vicinity of the Columbia River are long, parallel ridges (Cooper, 1958).

Extra-tropical cyclones approach the coast from a general westerly direction with a maximum frequency in the winter (Cooper, 1958; National Marine Consultants, 1961a). Winds from these storms arrive from a northwest to a southwest direction, depending on where the center of the storm is located as it impinges on the coast, and develop most of the larger waves that reach the coast.

Oceanographic Conditions.-- An east-setting surface current between 40°N and 50°N, called the Subarctic Current, diverges in a broad zone well seaward of the Washington-Oregon coast to form the north-setting Alaska Current and the south-setting California Current (Sverdrup, Johnson, and Fleming, 1942, pp. 722-3; Barnes and Pacquette, 1957; Tully and Barber, 1961). During the winter a north-setting surface counter-current, the Davidson Current, develops along the west coast of the United States to about 48°N. A subsurface counter-current is thought to be present during most of the year (Sverdrup, Johnson, and Fleming, 1942, p. 725) and is

exposed on the surface as the north-setting Davidson Current during the winter. The current is obscured during the rest of the year by upwelling of near-surface waters. All of these currents have low velocities and are located some distance offshore from the beach zone.

The Subarctic Current has the characteristics of a warm water mass and, as such, has an influence on the climatic conditions that exist along the coast. The climate, in turn, affects the vegetation, run-off, and ability of wind to transport sediment.

Wave action is a primary force to be considered when dealing with nearshore sediment distribution (Johnson, 1956). Several workers have attempted to estimate longshore current velocities by relating observed sediment movement in the littoral zone to wave momentum or energy and the angle of wave approach to the beach (Putnam, Munk, and Traylor, 1949; Handin and Ludwick, 1950; Watts, 1953; Caldwell, 1956). Watts and Caldwell used two somewhat different methods of relating wave energy flux to mass transport of sediments in a natural environment, and obtained similar results. Putnam et al. (1949) formulated a relationship derived from theoretical considerations among longshore current velocity, height, and period of breaking waves, angle between breakers and beach, and the beach slope. The derivations were based both on energy flux and momentum relationships. Their equations generally tend to give longshore current velocities that are too high (Bruun, 1963).

The wave regime off the Washington-Oregon coast has a definite seasonal character, as does the wind regime. The predominant direction of wave approach is from the northwest during the summer months, and from the southwest in the winter months. Almost all major storms come from the southwest (Lockett, 1962).

Wave measurements made from the Columbia River light vessel during the years 1933-1936, compiled by O'Brien (1948, 1951) show that the predominant wave direction was from west to southwest. He believed that sediment accretion after construction of the south jetty of the Columbia River was the result of an adjustment to an equilibrium alignment perpendicular to the predominant direction of wave attack.

National Marine Consultants (1961b) have compiled deep-water wave statistics at several locations off the Washington-Oregon coast for the years 1956, 1957, and 1958. They applied hindcasting methods of Pierson, Neumann, and James (1953) to determine significant wave heights and periods, and presented these values in tabular form as height-direction-period frequencies. They assume that this period represents average conditions. In another publication (National Marine Consultants, 1961a), wave refraction diagrams were constructed in order to evaluate wave energy characteristics near the mouth of the Columbia River. These data are presented in such a way that wave energy values may be computed for a given set of deep-water wave characteristics.

FIELD WORK

A sampling plan was developed by combining the natural zonation exhibited by a beach with an arbitrarily selected set of boundaries (Krumbein and Slack, 1956). Seventeen beach profiles and seven channel locations were sampled during the latter part of the summer (August, 1961) and of the winter (March, 1962) seasons. Nine additional samples were obtained at areas of special interest (Figure 6). Channel samples were obtained near channel-marker buoys at variable depths. Inclement weather prevented complete sampling of the Grays Harbor area. A major shift in the channel location at Willapa Bay precluded station reoccupation for determination of seasonal sediment changes.

Three sample points on the typical beach profile (Figure 7) were selected for study, the trough, 20-foot, and 30-foot locations. This follows a procedure described by Krumbein and Slack (1956) with sample-point density modifications due to the large area involved in the study. A total of 125 samples was selected for the study.

The 20- and 30-foot samples were obtained by use of a modified Van Veen grab sampler (.0064 cubic meters) and the trough samples were collected by swimmers using 2-5/16 inch (5.9 cm) plastic tubes. The samples were placed in plastic bags and stored for laboratory analyses.

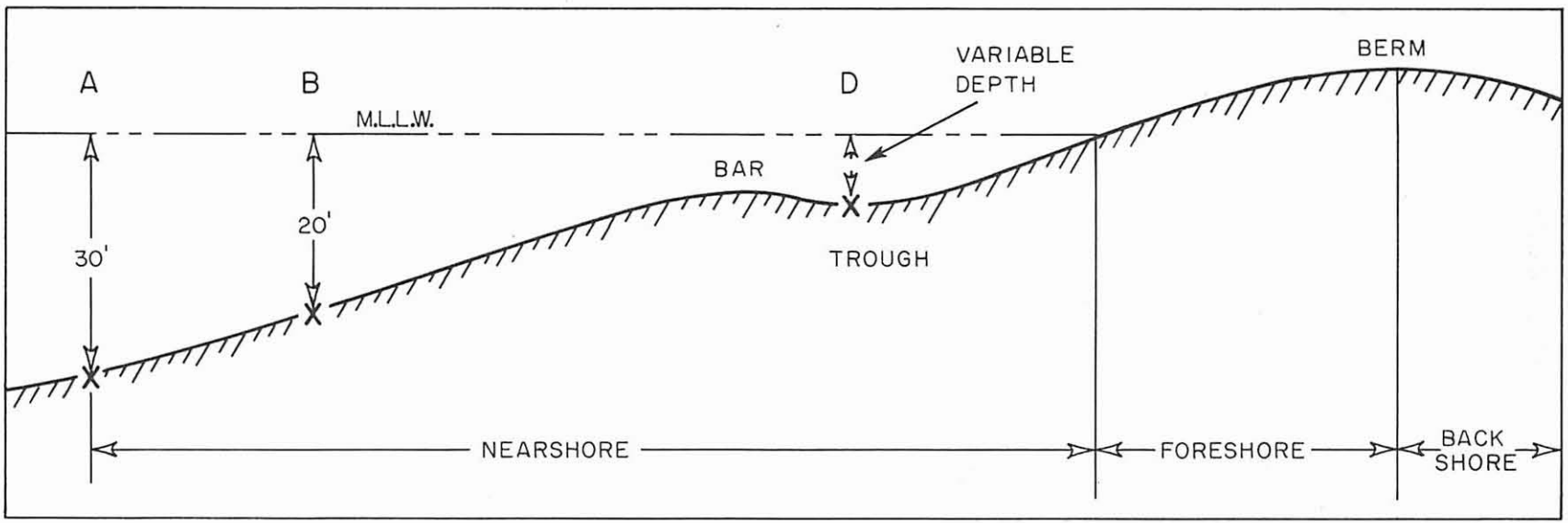

Fig. 7: Typical beach cross-section showing sample locations and beach nomenclature (after Krumbein and Slack, 1956).

ANALYTICAL METHODS AND PRESENTATION OF DATA

Texture and Composition of Sediments

The grain-size distribution of each sediment sample (Figure 6) was determined by means of a mechanical analysis. A split portion of each sample was size-graded using 8-inch sieves (W. S. Tyler Company, Cleveland, Ohio) with screen sizes that followed a 0.5 phi unit progression (Appendix III). Duplicate analyses resulted in a precision of about 0.1 to 0.2 phi units in the 2.0 to 3.0 phi-size range.

Size statistics were determined using a computer program (Creager, McManus, and Collias, 1962). Inman (1952) statistics were selected from the program results and utilized in this study. These values were condensed from the original program and are presented in Table I. A full set of size data is available on request at the Department of Oceanography, University of Washington.

A heavy mineral analysis was carried out on the 3.0 to 3.5 phi fraction of each sample to determine the abundance of heavy and magnetic minerals (Appendix II). Individual mineral frequencies were determined for a suite of the most common minerals at selected points.

Mean Grain-Size.-- The distribution of mean grain-size of the beach sediments is graphically presented in Figure 8. The grain-size values for each station were determined by averaging the mean grain-sizes of the trough, 20-foot, and 30-foot samples.

Seasonal variations of mean grain-size were generally small, about 0.1 phi unit (Figure 8), which would normally be ignored as within the experimental error of the method. However, the consistency of the variations were pronounced over long portions of the beach, and one is tempted to speculate

TABLE I

SAMPLE LOCATIONS AND SIZE STATISTICS ACCORDING TO INMAN (1952)

THE LETTERS A, B, AND D SIGNIFY THE SAMPLE LOCATION IN THE TYPICAL BEACH CROSS-SECTION, MEANING 30-FOOT, 20-FOOT, AND TROUGH RESPECTIVELY (FIGURE 7)

CRUISE 3-10

STA	LAT	LONG	SAND, SILT RELATIONSHIPS				INMAN VALUES		
			LARGER	SAND	SILT	SAND/SILT	MEAN	DEV	SKEW
1-A	45-57.9 N	123-56.0 W	0.00	98.58	1.41	69.91	2.96	0.27	0.11
1-B	45-57.9 N	123-56.0 W	0.00	97.26	2.70	36.02	2.91	0.30	0.17
1-D	45-57.9 N	123-06.0 W	0.00	98.84	1.13	87.47	2.27	0.44	-0.39
2-A	46-02.0 N	123-05.5 W	0.00	98.93	1.05	94.22	2.94	0.24	0.08
2-B	46-02.0 N	123-05.5 W	0.00	98.83	1.14	86.69	2.84	0.19	-0.37
2-D	46-02.0 N	123-05.5 W	0.00	99.16	0.82	120.93	2.24	0.35	-0.20
3-A	46-05.8 N	123-56.1 W	0.00	98.97	1.01	97.99	2.94	0.20	-0.15
3-B	46-05.8 N	123-56.1 W	0,00	98.98	1.00	98.98	2.73	0.33	-0.18
3-D	46-05.8 N	123-56.1 W	0.00	99.07	0.89	111.31	2.13	0.39	0.03
4-D	46-09.1 N	123-57.7 W	0.00	99.09	0.88	112.60	2.16	0.46	0.15
5-A	46-10.7 N	123-58.7 W	0.00	98.78	1.20	82.32	2.98	0.34	-0.09
5-B	46-10.7 N	123-58.7 W	0.00	98.79	1.19	83.02	2.89	0.45	-0.09
5-D	46-10.7 N	122-58.7 W	0.00	99.24	0.74	134.11	2.43	0.38	0.05
6-A	46-13.2 N	124-00.5 W	0.00	98.55	1.42	69.40	2.73	0.51	-0.18
6-B	46-13.2 N	124-00.5 W	0.00	98.80	1.16	85.17	2.74	0.40	-0.30
6-D	46-16.0 N	124-05.2 W	0.00	99.22	0.76	130.55	2.41	0.40	0.03
7-A	46-13.5 N	124-07.0 W	0.00	97.41	2.59	37.55	2.71	0.62	0.05
8-A	46-14.3 N	124-05.7 W	0.00	98.99	0.98	101.01	2.19	0.40	0.13
9-A	46-14.8 N	124-08.2 W	0.00	98.32	1.65	59.59	2.57	0.45	0.13

TABLE I (CONT)

CRUISE 3-10

STA	LAT	LONG	SAND, SILT RELATIONSHIPS LARGER	SAND	SILT	SAND/SILT	INMAN VALUES MEAN	DEV	SKEW
10-A	46-15.2 N	123-06.0 W	0.00	89.97	10.01	8.99	2.72	0.55	0.44
11-A	46-15.9 N	124-07.8 W	0.00	98.73	1.24	79.62	2.59	0.47	0.00
11-B	46-16.1 N	124-05.9 W	0.00	99.01	0.96	103.14	2.37	0.42	0.14
11-D	46-16.0 N	124-05.2 W	0.00	99.39	0.58	171.36	2.24	0.28	0.11
12-A	46-17.7 N	124-04.5 W	0.00	89.12	10.84	8.22	3.18	0.55	0.29
12-B	46-17.7 N	124-04.5 W	0.00	97.99	1.97	49.74	2.28	0.34	0.06
12-D	46-17.7 N	124-04.5 W	0.00	99.39	0.57	174.37	1.90	0.20	-0.25
13-A	46-21.2 N	124-03.5 W	0.00	99.08	0.91	108.88	2.22	0.29	0.03
13-B	46-21.2 N	124-03.5 W	0.00	99.09	0.88	112.60	2.19	0.33	0.00
13-D	46-21.2 N	124-03.5 W	0.00	99.43	0.55	180.78	2.08	0.29	-0.03
14-A	46-24.2 N	124-03.3 W	0.00	97.17	2.80	34.70	2.96	0.30	0.10
14-B	46-24.2 N	124-03.3 W	0.00	99.08	0.89	111.33	2.26	0.28	0.00
14-D	46-24.2 N	124-03.3 W	0.00	99.22	0.76	130.55	2.22	0.31	0.00
15-A	46-29.4 N	124-03.5 W	0.00	98.79	1.21	81.63	2.99	0.22	0.18
15-B	46-29.4 N	124-03.5 W	0.00	98.87	1.12	88.28	2.67	0.31	0.06
15-D	46-29.4 N	124-03.5 W	0.00	99.03	0.93	106.48	2.21	0.32	0.03
16-A	46-32.8 N	124-03.6 W	0.00	98.85	1.12	88.26	3.00	0.23	0.17
16-B	46-32.8 N	124-03.6 W	0.00	99.12	0.86	115.26	2.76	0.29	0.03
16-D	46-32.8 N	124-03.6 W	0.00	99.10	0.88	112.61	2.34	0.32	0.03
17-A	46-36.1 N	124-03.8 W	0.00	98.86	1.11	89.06	2.63	0.24	0.00
17-B	46-36.1 N	124-03.8 W	0.00	98.91	1.06	93.31	2.60	0.29	0.07
17-D	46-36.1 N	124-03.8 W	0.00	98.85	1.16	85.22	2.48	0.21	-0.14

TABLE I (CONT)

CRUISE 3-10

STA	LAT	LONG	SAND, SILT RELATIONSHIPS LARGER	SAND	SILT	SAND/SILT	INMAN VALUES MEAN	DEV	SKEW
19-A	46-40.0 N	124-06.8 W	0.00	98.54	1.45	67.96	2.72	0.26	0.04
20-A	46-41.8 N	124-06.4 W	0.00	98.97	1.00	98.97	2.54	0.24	-0.04
21-A	46-43.0 N	124-05.2 W	0.00	99.32	0.65	152.80	2.38	0.18	-0.28
22-D	46-43.4 N	124-04.7 W	0.00	99.45	0.51	195.00	2.37	0.31	-0.32
23-A	46-44.8 N	124-05.6 W	0.00	99.18	0.80	123.98	2.70	0.24	0.17
23-B	46-44.8 N	124-05.6 W	0.00	99.12	0.83	119.42	2.61	0.23	0.13
23-D	46-44.8 N	124-05.6 W	0.00	98.99	0.98	101.01	2.47	0.18	-0.11
24-A	46-47.8 N	124-05.9 W	0.00	99.08	0.89	111.33	2.77	0.22	0.14
24-B	46-47.8 N	124-05.9 W	0.00	99.18	0.78	127.15	2.59	0.27	-0.19
24-D	46-47.8 N	124-05.9 W	0.00	99.18	0.80	123.98	2.18	0.46	-0.20
25-A	46-51.6 N	124-06.8 W	0.00	98.94	1.03	96.06	2.91	0.24	0.04
25-B	46-51.6 N	124-06.8 W	0.00	99.11	0.87	113.92	2.76	0.25	-0.04
25-D	46-51.6 N	124-06.8 W	0.00	99.07	0.89	111.31	2.28	0.38	-0.11
26-A	46-54.0 N	124-07.8 W	10.54	88.76	0.70	142.16	2.27	0.71	-0.63
26-B	46-54.0 N	124-07.8 W	3.25	95.89	0.80	123.93	2.70	0.28	-0.21
26-D	46-54.0 N	124-08.0 W	34.54	65.01	0.46	217.45	0.39	2.22	0.38
28-A	46-55.8 N	124-10.2 W	0.00	99.24	0.72	137.83	2.37	0.44	-0.16
28-B	46-55.8 N	124-10.2 W	0.00	99.21	0.76	130.54	2.50	0.39	-0.15
28-D	46-55.9 N	124-10.2 W	3.11	96.08	0.81	122.72	1.74	0.49	-0.08
29-D	46-58.3 N	124-10.0 W	0.69	98.29	1.02	96.96	2.04	0.48	-0.14
30-D	47-01.2 N	124-10.0 W	0.00	98.83	1.17	84.60	2.61	0.25	0.03

TABLE I (CONT)

CRUISE 4-10

STA	LAT	LONG	SAND, SILT RELATIONSHIPS LARGER	SAND	SILT	SAND/SILT	INMAN VALUES MEAN	DEV	SKEW
1-A	45-57.9 N	123-06.0 W	0.00	98.36	1.64	59.97	2.60	0.26	0.04
1-B	45-57.9 N	123-06.0 W	0.00	98.83	1.17	84.42	2.66	0.27	0.00
1-D	45-57.9 N	123-06.0 W	0.00	98.99	1.01	98.50	2.48	0.31	-0.15
2-A	46-02.0 N	123-05.5 W	0.00	98.89	1.11	88.73	2.90	0.26	0.15
2-B	46-02.0 N	123-05.5 W	0.00	98.88	1.12	88.39	2.81	0.27	0.08
2-D	46-02.0 N	123-05.5 W	0.00	99.26	0.74	134.67	2.21	0.37	-0.01
3-A	46-05.8 N	123-56.1 W	0.00	98.57	1.43	68.82	2.92	0.25	-0.01
3-B	46-05.8 N	123-56.1 W	0.00	99.03	0.97	102.37	2.58	0.39	-0.06
3-D	46-05.8 N	123-56.1 W	0.00	99.24	0.76	131.35	2.15	0.28	0.08
4-D	46-09.1 N	123-57.7 W	0.00	99.18	0.82	121.33	2.08	0.27	0.03
5-A	46-10.7 N	123-58.7 W	0.00	98.61	1.39	71.04	3.02	0.40	0.04
5-B	46-10.7 N	123-58.7 W	0.00	98.99	1.01	97.60	2.99	0.43	0.01
5-D	46-10.7 N	123-58.7 W	0.00	99.38	0.62	160.44	2.31	0.31	0.00
6-A	46-13.2 N	124-00.5 W	0.00	98.71	1.29	76.74	2.93	0.47	-0.11
6-B	46-13.2 N	124-00.5 W	0.00	99.12	0.88	113.12	2.78	0.50	-0.14
6-D	46-16.0 N	124-05.2 W	0.00	99.27	0.73	135.40	2.30	0.33	0.10
7-A	46-13.5 N	124-07.0 W	0.00	98.28	1.72	57.12	2.72	0.39	0.04
8-A	46-14.3 N	124-05.7 W	0.00	98.55	1.45	67.76	2.38	0.38	0.15
9-A	46-14.8 N	124-08.2 W	0.00	98.52	1.48	66.55	2.46	0.36	0.11
10-A	46-15.2 N	124-06.1 W	0.00	98.92	1.08	91.35	2.23	0.42	-0.01

TABLE I (CONT)

CRUISE 4-10

STA	LAT	LONG	SAND, SILT RELATIONSHIPS LARGER	SAND	SILT	SAND/SILT	INMAN VALUES MEAN	DEV	SKEW
11-A	46-15.9 N	124-07.8 W	0.00	98.79	1.21	81.33	2.79	0.31	-0.05
11-B	46-16.1 N	124-05.9 W	0.00	99.17	0.83	119.05	2.49	0.43	0.19
11-D	46-16.0 N	124-05.2 W	0.00	99.65	0.35	288.40	2.33	0.28	0.15
12-A	46-17.7 N	124-04.5 W	0.00	98.23	1.77	55.43	2.53	0.26	0.10
12-B	46-17.7 N	124-04.5 W	0.00	98.48	1.52	64.58	2.26	0.26	-0.04
12-D	46-17.7 N	124-04.5 W	0.00	99.45	0.55	182.33	2.19	0.25	0.08
13-A	46-21.2 N	124-03.5 W	0.00	99.10	0.90	110.56	2.42	0.24	0.00
13-B	46-21.2 N	124-03.5 W	0.00	98.80	1.20	82.26	2.27	0.30	0.10
13-D	46-21.2 N	124-03.5 W	0.00	99.52	0.48	205.97	1.98	0.25	-0.13
14-A	46-24.2 N	124-03.3 W	0.00	90.30	9.70	9.31	3.01	0.37	0.48
14-B	46-24.2 N	124-03.3 W	0.00	98.95	1.05	94.40	2.55	0.28	0.03
14-D	46-24.2 N	124-03.3 W	0.00	98.89	1.11	88.91	1.94	0.23	-0.27
15-A	46-29.4 N	124-03.5 W	0.00	95.18	4.82	19.75	3.01	0.28	0.31
15-B	46-29.4 N	124-03.5 W	0.00	98.91	1.09	90.68	2.79	0.28	0.21
15-D	46-29.4 N	124-03.5 W	0.00	99.10	0.90	110.73	2.28	0.30	0.05
16-A	46-32.8 N	124-03.6 W	0.00	98.48	1.52	64.73	2.97	0.23	0.21
16-B	46-32.8 N	124-03.6 W	0.00	99.04	0.96	102.80	2.89	0.23	0.07
16-D	46-32.8 N	124-03.6 W	0.00	99.14	0.86	115.62	2.31	0.27	0.09
17-A	46-36.1 N	124-03.8 W	0.00	98.74	1.26	78.44	2.86	0.26	0.16
17-B	46-36.1 N	124-03.8 W	0.00	99.04	0.96	103.63	2.75	0.26	0.20
17-D	46-36.1 N	124-03.8 W	0.00	99.20	0.80	124.19	2.32	0.30	-0.04
18-D	46-38.6 N	124-02.0 W	0.00	99.20	0.80	123.50	2.31	0.31	0.03

TABLE I (CONT)

CRUISE 4-10

STA	LAT	LONG	SAND, SILT RELATIONSHIPS LARGER	SAND	SILT	SAND/SILT	INMAN VALUES MEAN	DEV	SKEW
19-A	46-40.0 N	124-06.8 W	0.00	98.69	1.31	75.24	2.60	0.20	0.19
22-D	46-43.7 N	124-04.7 W	0.00	99.18	0.82	121.02	2.46	0.21	-0.22
23-A	46-44.8 N	124-05.6 W	0.00	96.79	3.21	30.13	2.77	0.27	0.28
23-B	46-44.8 N	124-05.6 W	0.00	98.84	1.16	84.94	2.62	0.21	0.04
23-D	46-44.8 N	124-05.6 W	0.00	99.07	0.93	106.30	2.31	0.32	-0.32
24-A	46-47.8 N	124-05.9 W	0.00	98.42	1.58	62.39	2.81	0.22	0.15
24-B	46-47.8 N	124-05.9 W	0.00	99.18	0.82	121.35	2.82	0.24	0.07
24-D	46-47.8 N	124-05.9 W	0.00	99.08	0.92	107.29	2.47	0.16	-0.22
25-A	46-51.6 N	124-06.8 W	0.00	98.92	1.08	91.67	2.89	0.23	0.03
25-B	46-51.6 N	124-06.8 W	1.40	97.56	1.04	94.99	2.82	0.21	-0.21
25-D	46-51.6 N	124-06.8 W	0.00	99.11	0.89	111.64	2.44	0.23	-0.31
26-A	46-54.0 N	124-07.8 W	1.12	97.83	1.04	95.04	2.55	0.45	-0.43
26-B	46-54.0 N	124-07.8 W	0.00	99.15	0.85	116.96	2.72	0.24	-0.07
27-A	46-54.2 N	124-10.2 W	0.00	99.07	0.93	106.62	2.31	0.31	-0.01
28-A	46-55.8 N	124-10.2 W	0.53	99.04	0.43	231.37	1.26	0.77	0.46
28-B	46-55.8 N	124-10.2 W	0.00	99.22	0.78	127.11	2.43	0.49	-0.32
28-D	46-55.9 N	124-10.2 W	0.00	99.19	0.81	123.17	2.05	0.38	-0.11
29-A	46-57.7 N	124-09.9 W	0.00	97.11	2.89	33.66	2.95	0.29	0.12
29-B	46-57.7 N	124-09.9 W	0.00	98.50	1.50	65.66	3.03	0.16	0.33

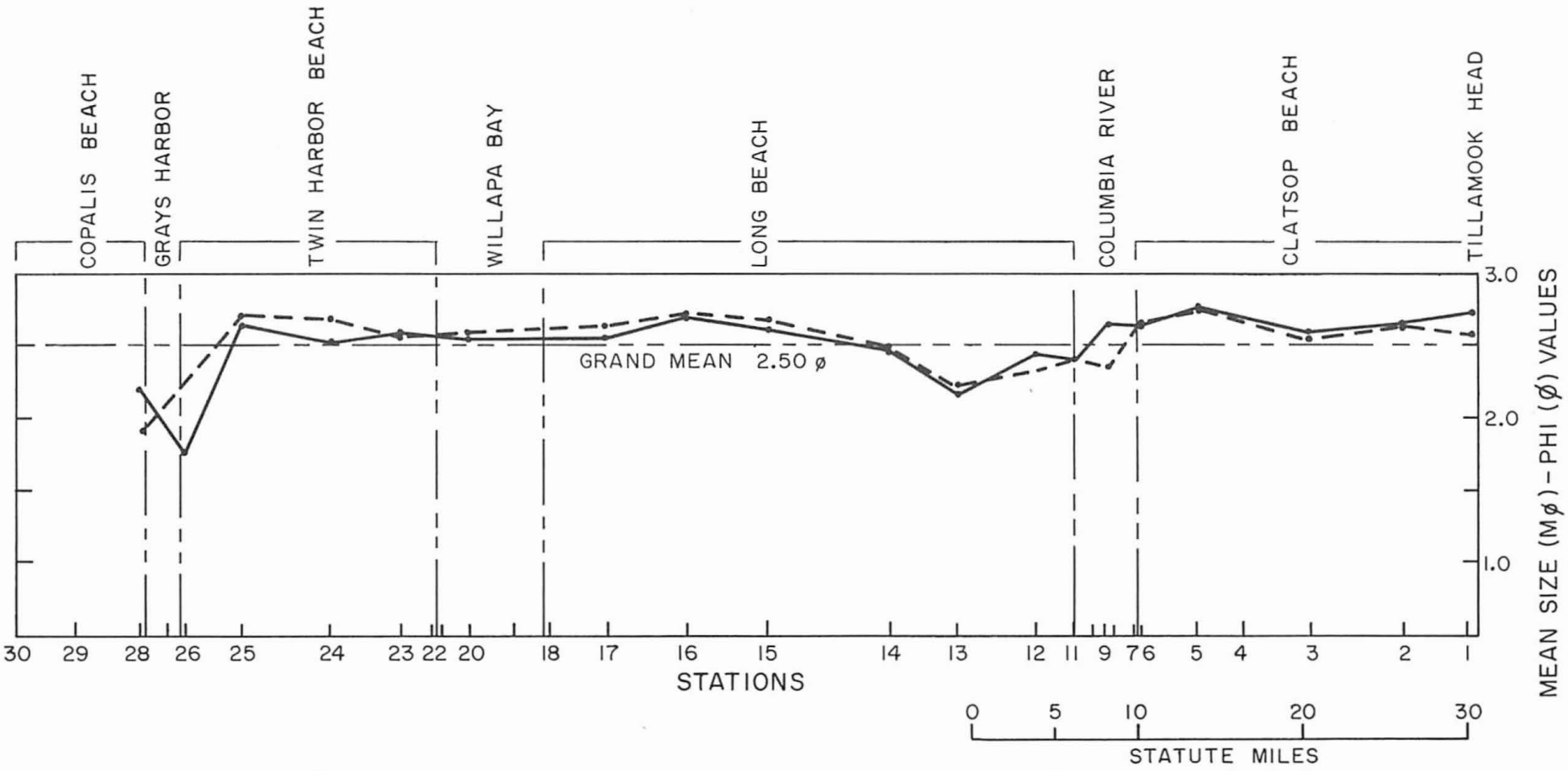

Fig. 8: Graph of seasonal variation of mean grain size (Mø). Trough, 20-foot, and 30-foot samples averaged for each station. The solid lines refer to samples obtained during summer conditions; the broken lines represent winter conidtions.

that the changes are significant. Clatsop Beach sediment is coarser in the winter, while the beach sediments north of the Columbia River generally have finer sediment during this season. These conditions suggest that the various beach zones may be subjected to different controlling factors.

The mean grain-size ($M\phi$) varies between 2.5 and 2.8 phi along the entire beach, except near Grays Harbor and the southern portion of Long Beach (Figure 8). Very little change in mean grain-size occurs across the Willapa Bay entrance. The mean grain-size of each beach zone was averaged ($\overline{M}$, Table II).

The variations in mean grain-size for the trough, 20-foot, and 30-foot samples are presented in Figure 9. The observed variations in each of these profiles in relation to its grand mean size is similar to that of Figure 8 except for somewhat greater variations at Willapa Bay in the 20-foot and 30-foot samples. Sediments were generally finer south of the Columbia River. Size variations are slight on both sides of Willapa Bay while sediment in the vicinity of Grays Harbor showed a wide seasonal variation. Trough samples were coarse on both sides of the Grays Harbor entrance in the summer. Samples from 30 feet showed much coarser sediment to the north during the winter.

Sorting.-- The variations in sorting coefficients ($\sigma\phi$, Inman, 1952) are graphically represented as a function of distance in Figure 10. The averaged sorting values for each beach zone are given in Table III, along with the standard deviations (s) of the samples from the mean value. The graphs and table show that the entire beach is composed of well-sorted sand except in the Grays Harbor area.

Folk and Ward (1957) group sediment sorting values into 5 types which

Table II: Averaged mean grain-size values ($\overline{M}_\phi$) for the various beach zones. Values are given in phi (ϕ) notation after Inman (1952).

Beach Zone		30-foot depth summer	30-foot depth winter	20-foot depth summer	20-foot depth winter	Trough summer	Trough winter	Grand Mean summer	Grand Mean winter
Clatsop Beach	$\overline{M}\phi$	2.91	2.87	2.82	2.76	2.27	2.26	2.67	2.63
	s[1]	.087	.144	.037	.140	.115	.129	.098	.137
Long Beach	$\overline{M}\phi$	2.74	2.71	2.48	2.55	2.21	2.18	2.48	2.48
	s	.322	.263	.214	.214	.152	.161	.243	.223
Twin Harbors Beach	$\overline{M}\phi$	2.66	2.76	2.67	2.75	1.94	2.42	2.43	2.64
	s	.239	.127	.069	.084	.780	.055	.503	.093
All[2] samples	$\overline{M}\phi$	2.75	2.68	2.62	2.65	2.15	2.24	2.49	2.51
Columbia River Samples								2.55	2.45

[1] s = the standard deviation. $s = \sqrt{\frac{\Sigma x^2}{n}}$

[2] Summed averages of all 30-foot, 20-foot, and trough samples.

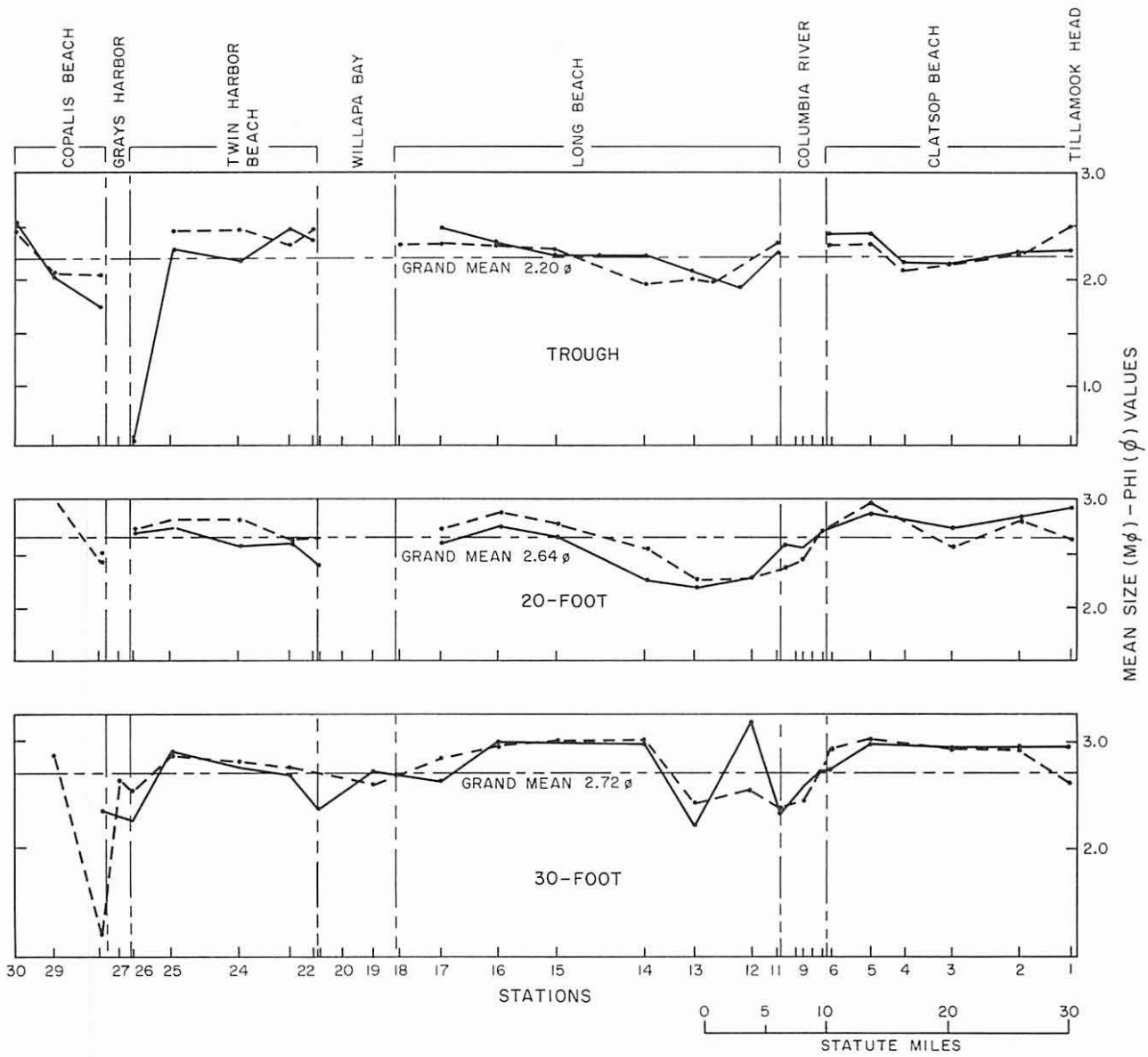

Fig. 9: Seasonal variations of mean grain size for the trough, 20-foot, and 30-foot samples. Values are given in phi (ϕ) notation. The solid lines represent samples obtained during the summer months; the broken lines represent winter conditions.

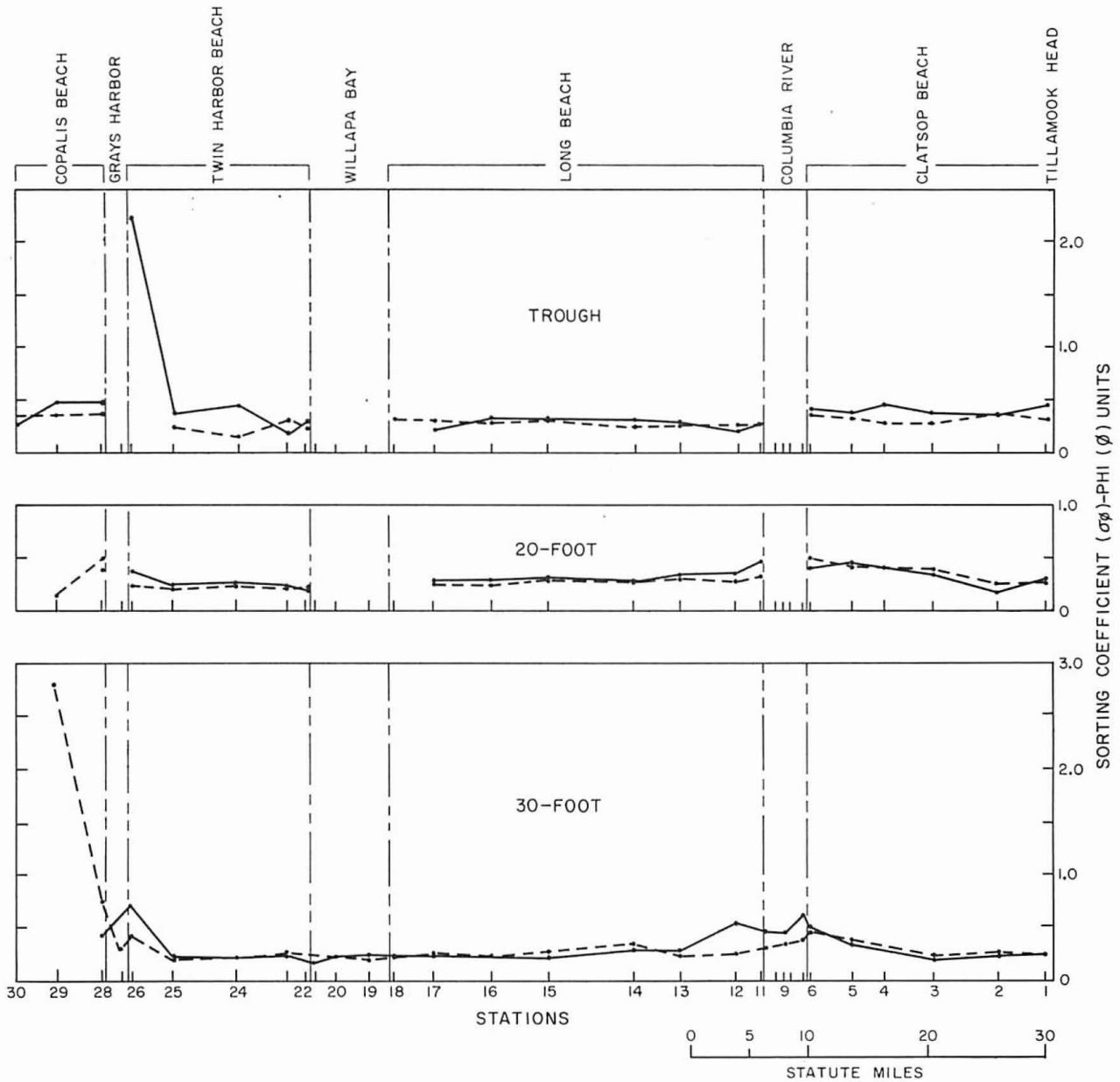

Fig. 10: Seasonal variations in sorting coefficients ($\sigma\phi$) along the beach for the trough, 20-foot, and 30-foot samples. Values are given in phi (ϕ) notation. The solid lines represent samples obtained during the summer months; the broken lines represent winter conditions.

Table III: Sorting values (σ_ϕ) for the various beach zones. Values given in phi (ϕ) notation after Inman (1952).

Beach Zone		30-foot depth summer	30-foot depth winter	20-foot depth summer	20-foot depth winter	Trough summer	Trough winter	Grand Mean summer	Grand Mean winter
Clatsop Beach	σ_ϕ	0.31	0.33	0.33	0.34	0.40	0.31	0.35	0.33
	s[1]	.110	.091	.091	.115	.034	.034	.082	.086
Long Beach	σ_ϕ	0.34	0.33	0.27	0.28	0.27	0.32	0.32	0.28
	s	.123	.066	.062	.027	.051	.026	.087	.044
Twin Harbors Beach	σ_ϕ	0.35	0.29	0.26	0.23	0.71	0.23	0.44	0.25
	s	.207	.074	.000	.000	.764	.057	.154	.063

[1] s = the standard deviation. $s = \sqrt{\frac{\Sigma x^2}{n}}$

describe the quality or degree of sorting, ranging from very well-sorted to very poorly-sorted. Ninety-five percent of the samples analyzed were in the very well- or well-sorted categories. Of the 42 samples from Long Beach 37 (88 percent) are very well-sorted.

Skewness.-- A graphical representation of the variation of skewness with distance was presented for both summer and winter conditions (Figure 11). The skewness values for sediment of Clatsop Beach decrease in the winter for almost all samples, while Long Beach does not follow this trend (Table IV). Its sediment generally becomes more positively skewed during the winter. Twin Harbors Beach exhibits a more random variation with seasons, indicating no particular trend. Insufficient data were available for a discussion of Copalis Beach.

Heavy Minerals.-- The results of the heavy mineral analyses (Appendix II) were plotted graphically for the trough, 20-foot, and 30-foot samples (Figure 12, Table V). Heavy mineral concentrations increase in the vicinity of the Columbia River, Willapa Bay, and Grays Harbor, with the greatest concentrations north of the Columbia River. The only significant increase of magnetic minerals is at, and immediately to the north of, the Columbia River. A slight increase is observed at Grays Harbor, but very little change was noted across the Willapa Bay entrance.

Variations of heavy mineral frequencies for the trough, 20-foot, and 30-foot samples were averaged for each beach station as were the channel samples for each entrance area (Figure 13). The highest values were just north of the Columbia River and Grays Harbor, while Willapa Bay showed a smaller increase. Magnetic minerals constituted approximately 1 percent of the beach sand throughout the study area except near Grays Harbor and the

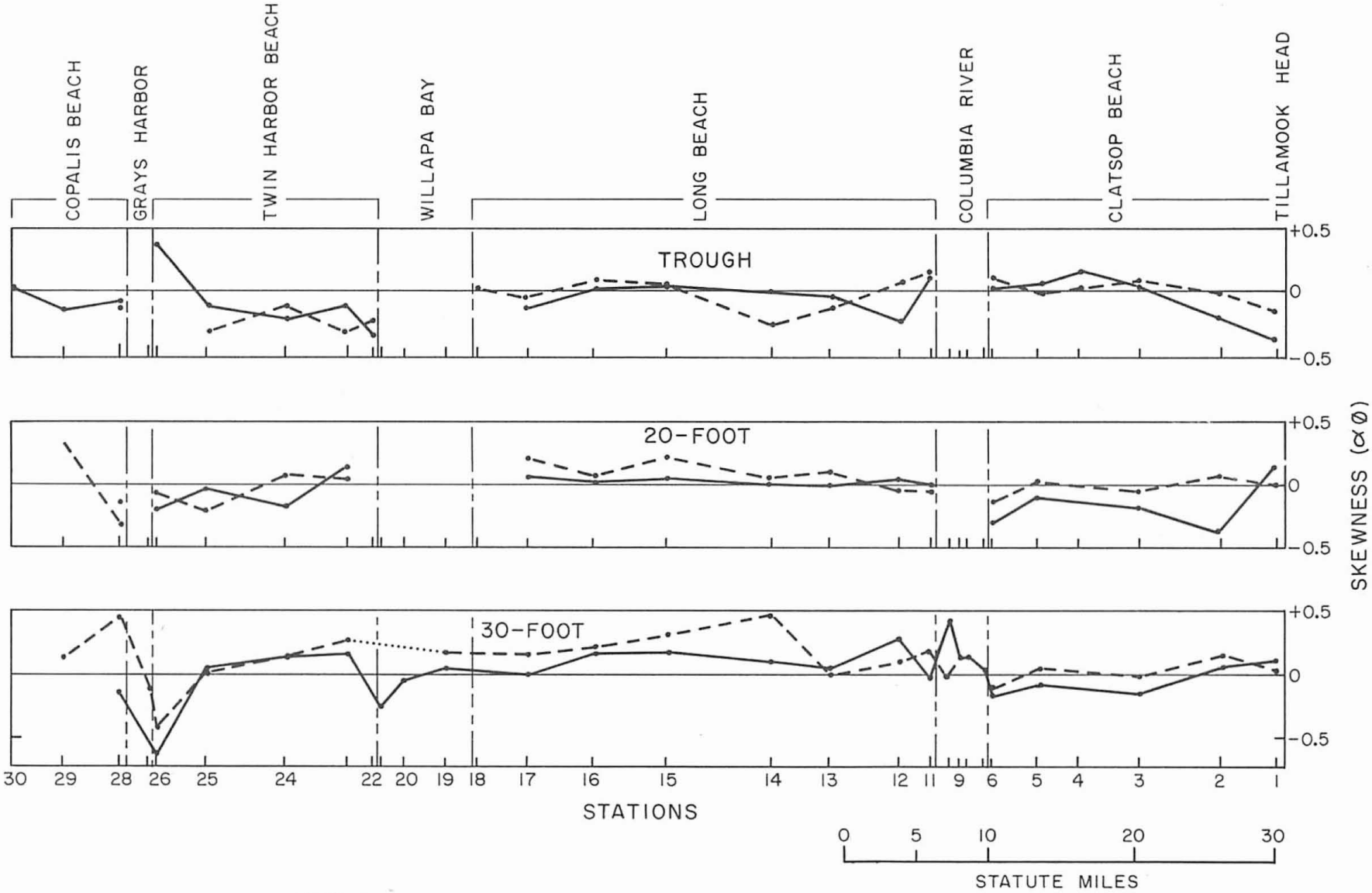

Fig. 11: Seasonal variations in skewness values ($\alpha\phi$) along the beach for the trough, 20-foot, and 30-foot samples. Values are given in phi (ϕ) notation. The solid lines represent samples obtained during summer conditions; the broken lines represent winter conditions.

Table IV: Skewness values (α_ϕ) for the various beach zones. Values given in phi (ϕ) notation after Inman (1952).

Beach Zone		30-foot depth summer	30-foot depth winter	20-foot depth summer	20-foot depth winter	Trough summer	Trough winter	Grand Mean summer	Grand Mean winter
Clatsop Beach	α_ϕ	-.05	.02	-.15	.04	-.06	.01	-.09	.02
	s[1]	.134	.095	.212	.167	.200	.089		
Long Beach	α_ϕ	.11	.18	.03	.07	-.04	-.01	.03	.08
	s	.100	.170	.032	.105	.122	.152		
Twin Harbors Beach	α_ϕ	-.07	.01	-.08	-.04	-.07	-.27	-.07	-.10
	s	.378	.300	.105	.127	.267	.063		

[1] s = the standard deviation. $s = \sqrt{\frac{\Sigma x^2}{n}}$

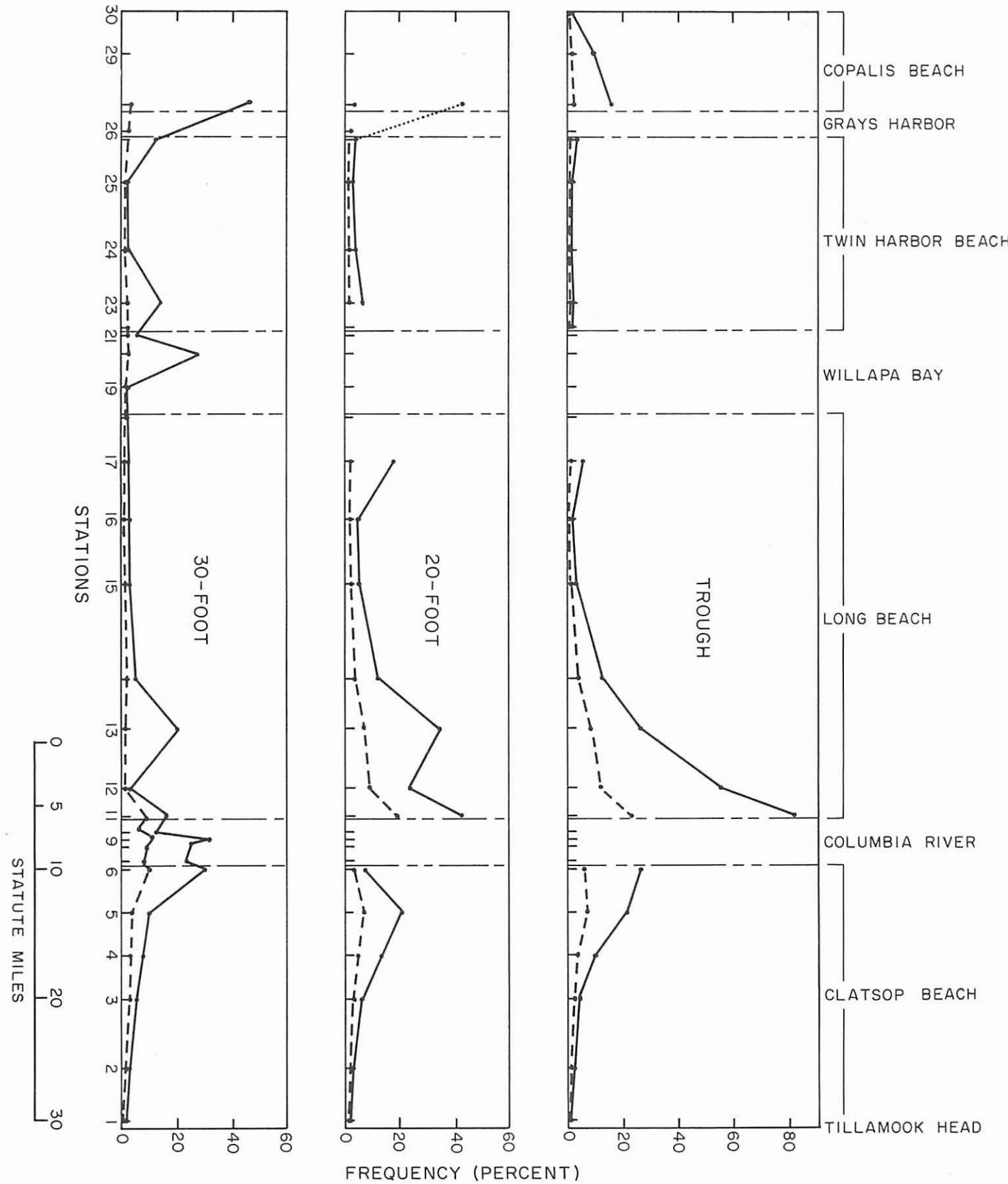

Fig 12: Variations of heavy magnetic minerals compared along the beach. Both are reported as "percent of total sample" in the 3.0 to 3.5 phi range. Heavy minerals are represented by solid lines and magnetic minerals by broken lines.

Table V: Relative frequencies of heavy and magnetic minerals for the study area. Values are given as "percent of total sample" in the 3.0 to 3.5 phi size range.

Sample	Heavy Minerals (%)	%	Magnetic Minerals (%)	%
1-A	2.3		1.2	
1-B	2.0	2.2	1.0	1.0
1-D	2.2		0.9	
2-A	2.9		1.5	
2-B	3.2	2.9	1.7	1.5
2-D	2.6		1.2	
3-A	4.6		2.4	
3-B	6.2	5.4	2.8	2.4
3-D	4.5		2.0	
4-D	9.7	9.7	4.0	4.0
5-A	9.9		4.0	
5-B	19.7	17.2	7.0	6.3
5-D	21.9		8.0	
6-A	29.9		9.8	
6-B	7.4	21.0	3.1	6.5
6-D	25.8		6.6	
7-A	22.2		7.9	
8-A	24.0	22.4	8.4	7.8
9-A	30.7		10.4	
10-A	11.7		4.1	
11-A	16.2		9.4	
11-B	41.6	46.5	18.8	17.1
11-D	81.7		23.2	
12-A	3.4		1.6	
12-B	23.4	30.8	8.7	7.5
12-D	55.6		12.1	
13-A	20.2		1.7	
13-B	33.1	26.8	7.4	6.1
13-D	26.8		9.2	
14-A	5.4		2.1	
14-B	11.3	9.9	4.0	3.5
14-D	12.5		4.4	
15-A	2.8		1.3	
15-B	5.1	4.1	2.1	1.7
15-D	4.4		1.8	
16-A	2.7		1.0	
16-B	5.0	3.3	1.8	1.3
16-D	2.2		1.0	
17-A	2.6		1.1	
17-B	16.5	8.5	1.7	1.4
17-D	6.4		1.3	
18-D				
19-A	2.5		1.9	
20-A	27.6	9.3	2.6	1.6
21-A	5.4		1.4	
22-D	1.5		0.4	
23-A	13.7		2.1	
23-B	6.6	7.8	1.5	1.4
23-D	3.0		0.7	
24-A	3.0		0.8	
24-B	3.7	3.3	1.1	0.8
24-D	2.1		0.5	
25-A	2.1		0.6	
25-B	3.0	2.6	0.8	0.6
25-D	2.7		0.5	
26-A	12.9		1.5	
26-B	3.7	7.0	0.7	1.1
26-D	4.4		1.0	
27-A				
28-A	46.6		3.8	
28-B	42.6	34.9	2.6	3.0
28-D	15.6		2.5	
29-A				
29-B				
29-D	10.1	10.1	1.4	1.4
30-D	1.8	1.8	0.4	0.4

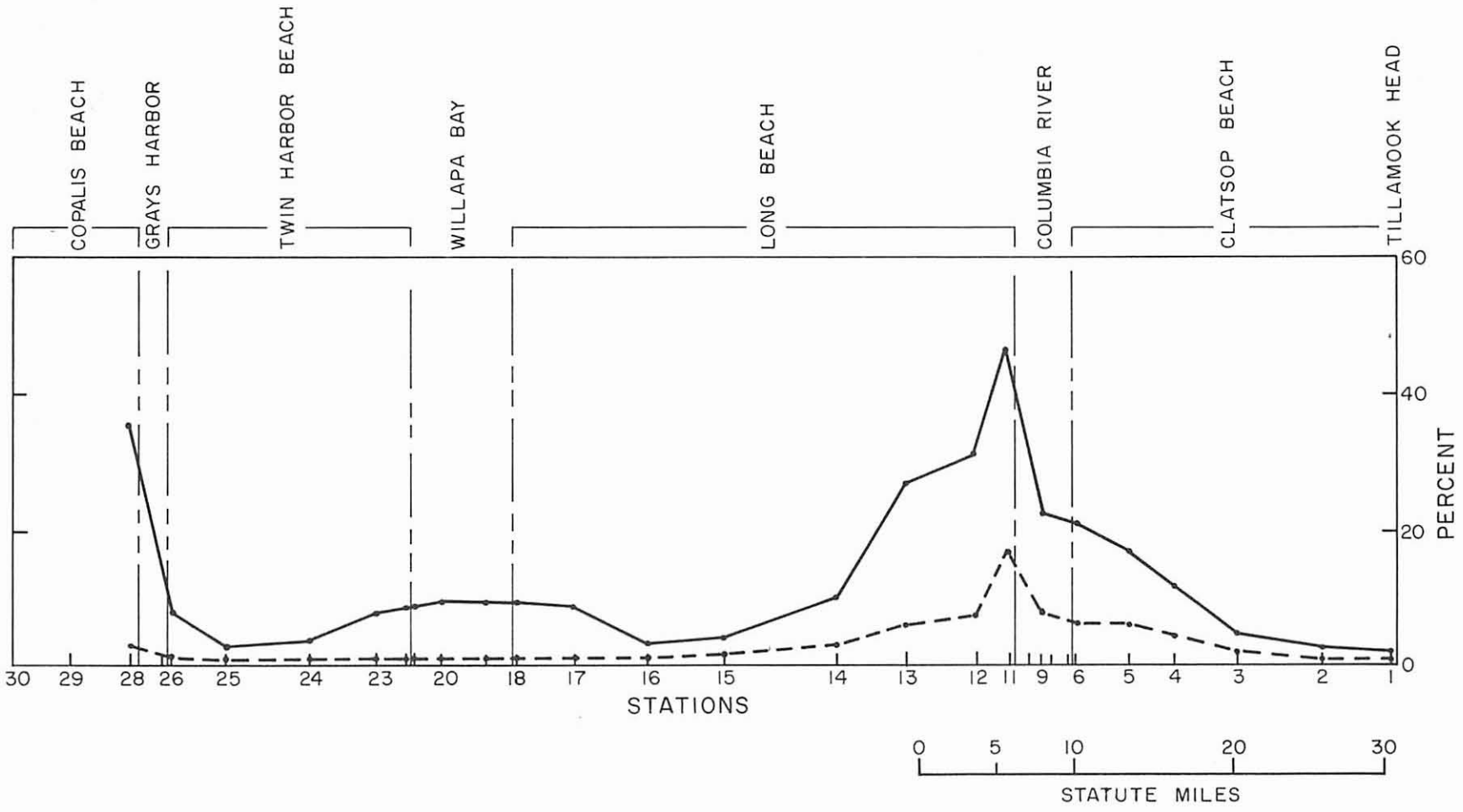

Fig. 13: Heavy and magnetic mineral variations for summer samples, averaged values. Values represent the 3.0 to 3.5 phi size range. The solid lines represent heavy minerals; the broken lines refer to magnetic minerals.

Columbia River (Figure 13). The highest values were again just north of these points. No increase was observed in the Willapa Bay area.

A suite of the most common heavy minerals was selected for individual frequency determinations (Table VI). Their relative variations were plotted as a function of distance (Figure 14). Hornblende was the only common heavy mineral that occurred with a fairly constant frequency so it was used as a base for ratio computations (Figure 15). The ratio of hypersthene to hornblende has highest values immediately north of the Columbia River and Willapa Bay. The ratio of other amphiboles (primarily tremolite-actinolite) to hornblende appeared to be inversely proportional to the hypersthene/hornblende ratio.

Waves

Steepness.-- Steepness values were determined for various combinations of wave heights and periods as reported by National Marine Consultants (1961b, Table 2.13) for a point about 20 miles (29 kilometers) west of the Columbia River (46°12'N, 124°30'W). Wave data were reported both for locally-formed wind waves at that point (termed seas), and for waves arriving at that point after being formed at another location (termed swells). The terms sea and swell will refer to the above definitions in the following discussion.

The steepness of a wave is defined as the ratio of the wave height to its length (H_o/L_o) and is a critical factor in determining its capacity to move sediment (Saville, 1950). The subscript "o" refers to wave values determined in deep water. Deep water is defined as water whose depth is greater than 1/2 the wave length of the wave in question, and it is assumed that boundary conditions of the bottom have no effect on waves at these depths.

Table VI: Relative percent of selected heavy minerals at various stations. The last two columns are the mineral ratios shown in Figure 15.

Sta	Hbl	Hyp	Other Amph	Mica	Cor	Iron Oxide	Oliv	Other	Hyp/Hbl	Other Amph/Hbl
1-A	9	1	21	42	3	19	2	3	.11	2.32
1-B	12	4	11	49	1	12	4	7	.33	.92
1-D	12	4	21	25	3	17	9	9	.33	1.75
5-A	39	13	14	8	6	3	7	10	.30	.36
5-B	44	20	12	1	11	--	7	9	.45	.27
5-D	46	19	17	1	2	1	3	10	.41	.37
7-A	37	28	11	2	4	1	9	8	.76	.30
9-A	33	28	13	2	8	--	4	12	.85	.40
11-A	24	34	3	6	6	1	6	20	1.42	.13
13-A	34	22	9	3	15	3	10	4	.65	.27
13-B	33	16	13	2	20	4	8	4	.49	.39
13-D	43	24	13	1	3	3	7	7	.56	.30
15-A	22	8	16	26	--	16	2	10	.36	.73
15-B	40	7	18	8	4	8	8	7	.18	.45
15-D	43	8	22	4	5	5	6	7	.19	.51
17-A	22	4	24	15	7	11	9	8	.18	1.01
17-D	40	7	20	4	20	2	7	--	.18	.50
19-A	29	4	13	25	3	7	11	9	.14	.45
20-A	33	5	16	17	6	6	8	9	.15	.49
21-A	25	23	9	7	18	3	9	6	.92	.36
23-A	32	15	11	2	18	3	12	7	.47	.34
23-B	36	12	11	8	10	2	8	13	.33	.31
23-D	40	7	23	6	2	3	8	11	.18	.58
24-A	23	9	13	15	9	12	12	7	.39	.57
24-B	32	9	16	7	7	6	16	7	.28	.50
24-D	41	11	16	5	7	9	7	4	.30	.39

Sta = Station
Hbl = Hornblende
Hyp = Hypersthene
Amph = Amphiboles (Primarily Actinolite and Tremolite)
Mica = Chlorite-Biotite-Muscovite
Cor = Corundum
Iron Oxide = Hematite-Limonite
Oliv = Olivine
Other = Remainder
Hyp/Hbl = Hypersthene/Hornblende
Other Amph/Hbl = Other Amphiboles/Hornblende

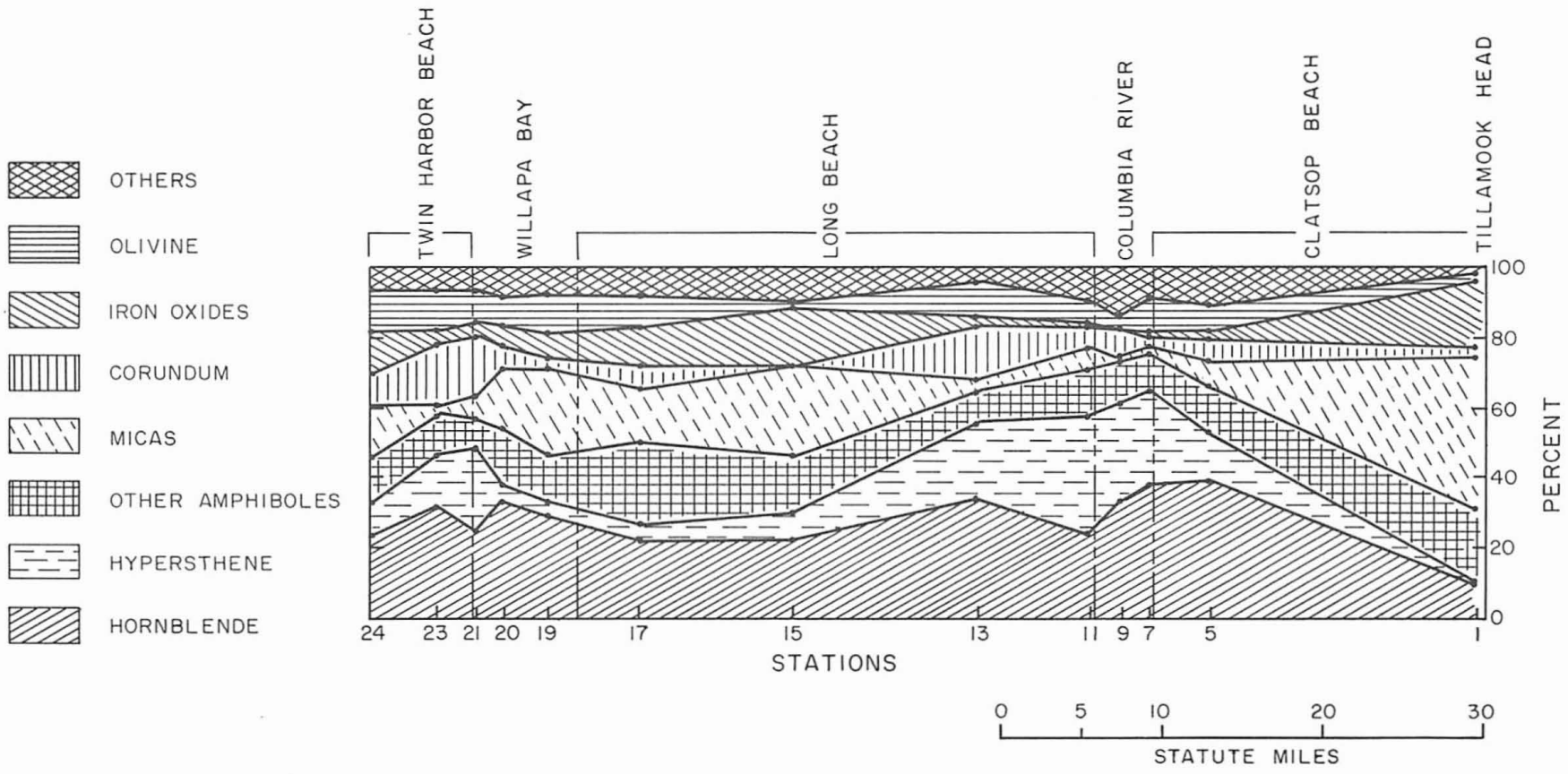

Fig. 14: The composition of a selected suite of heavy minerals as a function of distance along the beach. Minerals are of the 3.0 to 3.5 phi size range and represent only samples from the channels and the 30-foot depths.

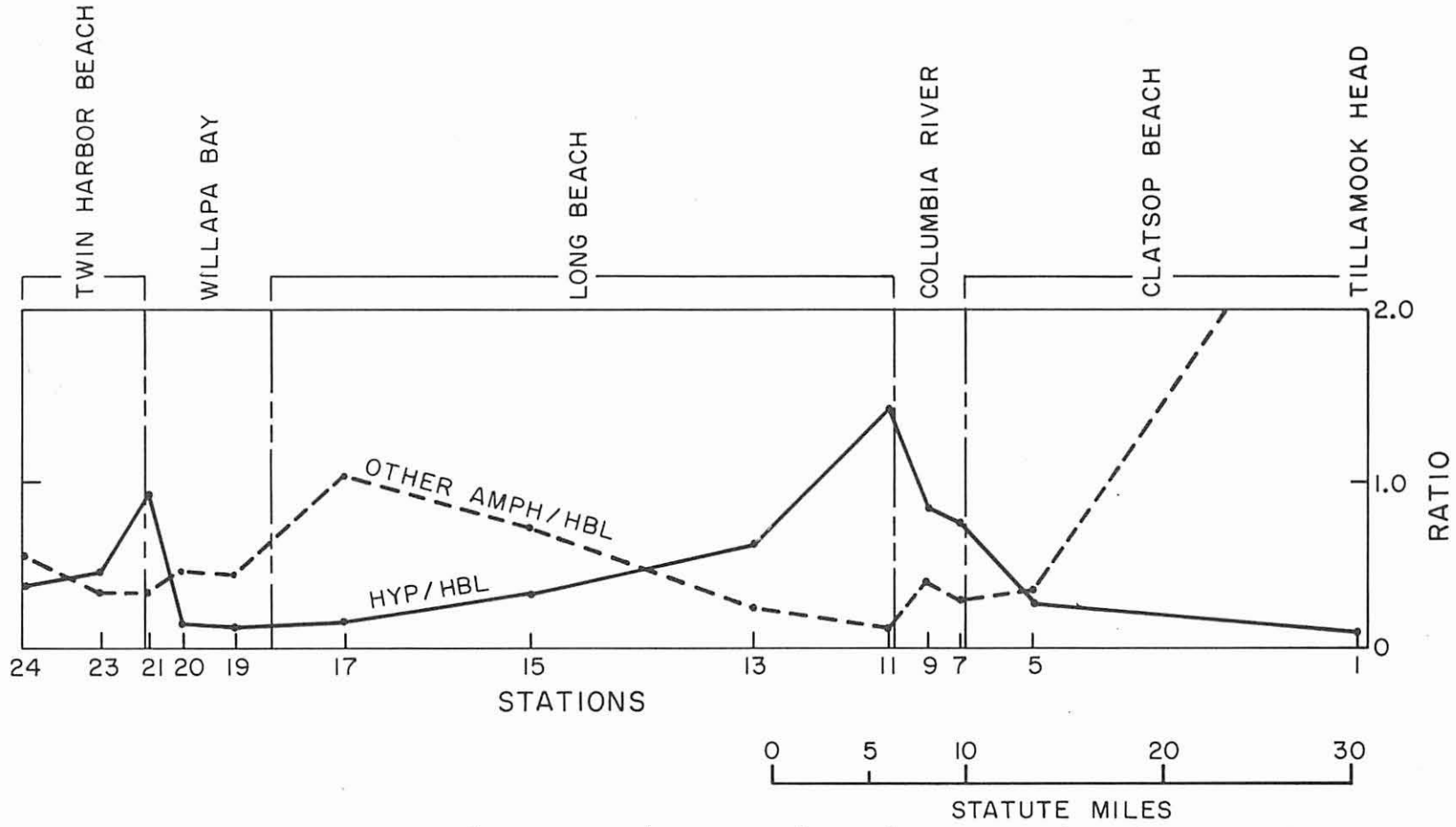

Fig. 15: Ratios of (Hypersthene/Hornblende) and (other Amphiboles/Hornblende) compared. "Other Amphiboles" include tremolite-actinolite as major contributors.

Values for wave heights were obtained directly from the wave statistics. The wave lengths were calculated from the wave periods by assuming that the waves could be treated as gravity waves. By means of classical hydrodynamics, the velocity of a wave can be expressed by the following (Sverdrup, Johnson, and Fleming, 1942):

$$c^2 = \frac{gL}{2\pi} \tanh \frac{2\pi d}{L}$$

where g = acceleration of gravity, L = wave length, and d = the depth of water. In deep water (deeper than 1/2 the wave length) tanh $2\pi d/L$ approaches the numerical value of one and the equation reduces to:

$$c^2 = \frac{gL_o}{2\pi} .$$

The velocity, period, and length of a wave are related by the expression (Fleming et al., 1942):

$$c = L/T .$$

By combining the last two equations and transposing the following expression is obtained (see Appendix I):

$$L_o = \frac{gT^2}{2\pi} .$$

This equation was substituted into the steepness equation (H_o/L_o) and the steepness value was determined for each set of wave statistics.

The steepness values were divided into three groups and the relative frequencies of occurrence in each group were determined for various wave directions (Table VII). When comparing the steepness values for seas and swells it was apparent that each one fell into a different group. Most of the swells (81.5 percent) fell in the H_o/L_o range of < 0.015 while seas were dominant (90.3 percent) in the 0.015 to 0.025 range.

Table VII: Relative frequency of waves with given steepness (H_o/L_o) values from various directions. Values represent average annual conditions for the years 1956, 1957, and 1958.

H_o/L_o	Cond.	Percent occurrence from various wave directions										
		N	NNW	NW	WNW	W	WSW	SW	SSW	S	SSE	Σ
<0.015	sea		-	-	-	-	-	-	0.1	-	-	0.1
	swell		0.6	9.0	24.2	26.4	10.2	4.7	4.0	2.3	0.1	81.5
0.015-0.025	sea	4.8	6.9	22.2	5.9	8.5	4.8	9.4	10.2	13.8	3.8	90.3
	swell	-	0.1	1.3	5.6	4.9	1.9	1.4	1.7	0.9	0.1	17.9
>0.025	sea	0.4	0.5	1.7	0.6	0.5	0.8	1.3	1.2	1.8	0.8	9.6
	swell	-	-	0.1	0.1	0.2	0.1	0.1	-	-	-	0.6

The relative frequencies of waves from various directions were graphically represented (Figure 16). Only waves with steepness values in the range 0.015 to 0.025 were considered as this range results in the greatest amount of sediment movement (Saville, 1950). The predominance of seas over swells in this steepness range is evident (Figure 16).

When summing up the relative frequencies of both seas and swells from north-of-west and from south-of-west, the results were nearly equal (inset, Figure 16). The apparent net effect on sediment movement would be to keep it localized according to these data.

Energy.-- Another method of determining the relative effects of various waves was by consideration of the wave energy relationships. The longshore component of wave energy flux was computed by Caldwell's (1956) method, with alterations required by the nature of the available data (Appendix I). The total energy of a water wave per unit length of wave crest may be approximated by (U.S. Army Corps of Engineers, 1961):

$$E_T = \frac{\rho g H^2 L}{8}$$

where ρ = density of water, g = acceleration of gravity, H = wave height, and L = wave length. The modifications that a wave undergoes as it passes through shoaling water may be approximated using a wave refraction diagram (Pierson, Neumann, and James, 1953). Wave refraction diagrams are available for waves of various periods and deep water directions for the shoreline in the immediate vicinity of the Columbia River (National Marine Consultants, 1961a). A point (Station 14, Figure 6) about 7 miles (10.1 kilometers) north of the Columbia River and another point (Station 3, Figure 6) about 7 miles (10.1 kilometers) south of the river were selected for the refraction

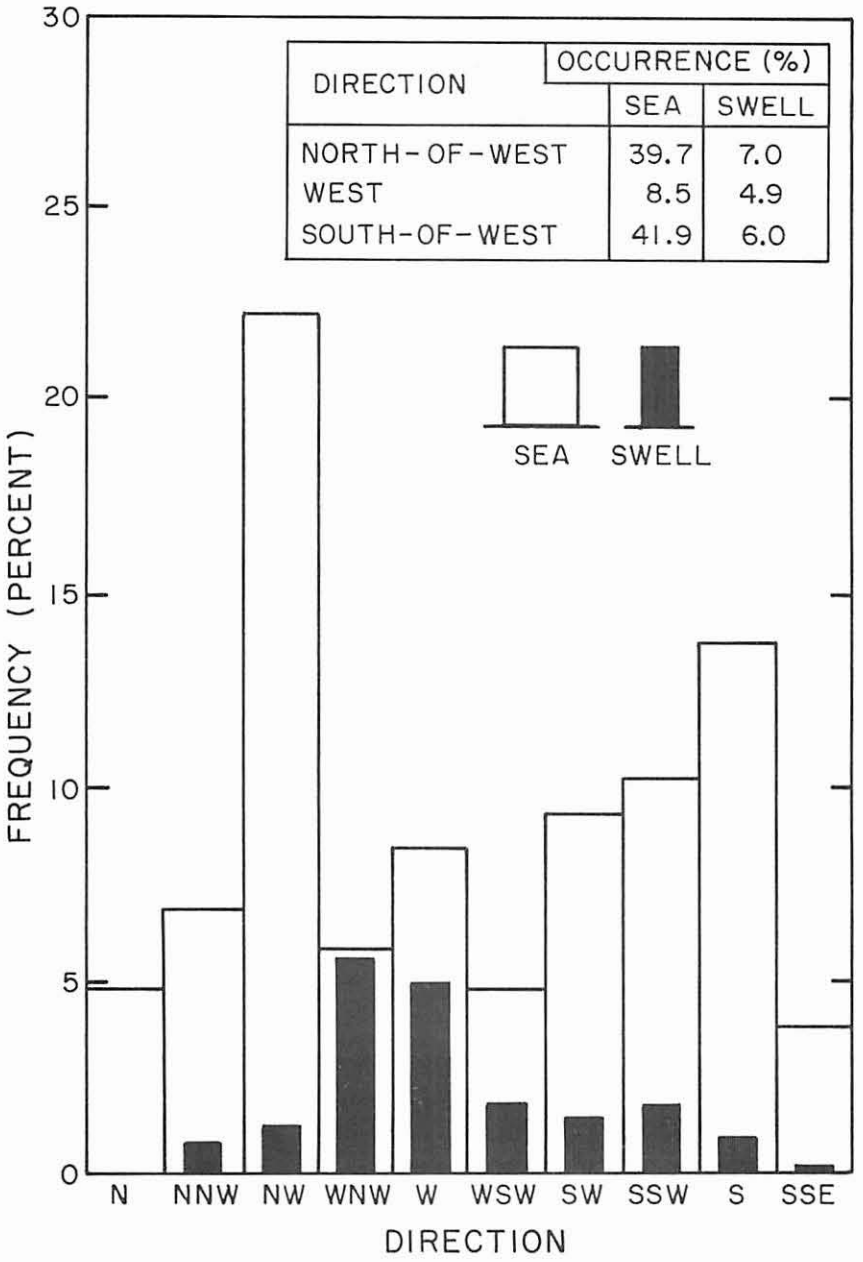

Fig. 16: Relative frequency and direction of deep-water waves with steepness values of H_o/L_o = 0.015 to 0.025. All values represent average annual wave conditions.

study. The energy coefficient (b_o/b) and angle (α) at which the wave crests impinge on the beach were determined for various wave periods and deep-water directions. The values obtained were substituted into an equation representing the longshore component of wave energy flux (Appendix I):

$$E_{(L.S.)} = 20.5\ H_o^2\ T(b_o/b)\ t \sin \alpha \cos \alpha\ dx$$

H_o = Deep-water wave height in feet

T = Wave period in seconds

b_o/b = Energy coefficient, or square of refraction coefficient

t = Time in seconds

α = Angle of incidence of shallow water wave crest on the beach

dx = Length of beach for which the angle of incidence was determined

Substituting the number of seconds per day for t, and one foot for dx, the longshore component of wave energy flux in foot-pounds per foot of beach per day is obtained for a given wave height and period.

Refracted wave crests with a longshore component to the north were assigned positive values and those with southerly components were given negative values. Energy flux values were computed for both sea and swell conditions and for monthly as well as annual increments (Table VIII). Monthly wave conditions south (Figure 17a) and north (Figure 18a) of the Columbia River appear quite similar, though the north station has values of greater magnitude. They both reflect a strong northerly energy flux in the winter (December-March) and a weaker southerly flux during summer (May-September).

By separating the monthly sea and swell energy-flux values a somewhat

TABLE VIII

LONGSHORE COMPONENT OF WAVE ENERGY FLUX FOR A POINT SOUTH (S) AND A POINT NORTH (N) OF THE COLUMBIA RIVER AS A RESULT OF SEAS AND SWELLS FROM THE GIVEN DIRECTIONS (FOOT LBS/FOOT OF BEACH/UNIT OF TIME)X(10)
(-) = FLUX TOWARD THE SOUTH

MONTH/DIRECTION			NNW	NW	WNW	W	WSW	SW	SSW	S	TOTAL
JAN	(SWELL)	N	0.000	-6.003	-21.250	13.397	33.453	16.230	16.067	0.680	52.573
		S	0.000	-1.991	-12.959	-11.307	17.774	12.902	15.260	0.692	20.371
	(SEA)	N	0.000	-6.979	-16.600	4.378	5.496	30.020	40.758	55.398	174.048
		S	0.000	-2.281	-8.907	-3.939	1.688	21.925	44.187	55.940	135.077
FEB	(SWELL)	N	-0.990	-9.750	-25.043	14.216	12.117	16.094	26.349	8.737	41.731
		S	-0.185	-3.446	-15.857	-11.277	5.943	12.081	24.751	9.117	21.127
	(SEA)	N	-0.438	-14.631	-13.053	5.904	9.919	12.487	36.428	29.053	65.668
		S	-0.038	-4.845	-11.067	-5.494	3.235	9.995	35.361	37.451	64.597
MAR	(SWELL)	N	-0.191	-4.737	-18.182	30.359	7.853	6.245	14.500	3.591	39.438
		S	-0.037	-1.558	-11.836	-24.673	3.618	5.324	16.473	4.366	-8.323
	(SEA)	N	-2.154	-3.932	-5.678	8.883	9.899	19.902	15.784	26.454	69.156
		S	-0.170	-1.126	-7.427	-7.920	3.316	16.505	20.071	36.961	60.211
APR	(SWELL)	N	0.000	-11.416	-19.485	6.667	26.408	0.385	1.417	0.260	4.235
		S	0.000	-3.842	-12.470	-5.716	14.094	0.318	1.813	0.295	-5.509
	(SEA)	N	-6.107	-28.810	-3.525	2.120	17.409	6.265	5.240	2.539	-4.868
		S	-0.422	-9.061	-4.403	-2.084	5.391	3.929	7.854	8.003	9.207
MAY	(SWELL)	N	0.000	-6.012	-17.797	7.598	3.640	0.410	3.342	0.041	-8.779
		S	0.000	-0.936	-11.551	-6.438	1.624	0.368	2.568	0.420	-13.945
	(SEA)	N	-15.172	-40.092	-0.712	1.266	0.465	2.839	2.018	5.537	-43.852
		S	-1.455	-12.898	-3.206	-1.256	0.080	1.934	3.292	7.375	-6.134
JUN	(SWELL)	N	0.000	-7.869	-11.519	9.807	2.331	3.036	0.000	0.000	-4.214
		S	0.000	-2.654	-7.863	-8.291	1.021	2.708	0.000	0.000	-15.079
	(SEA)	N	-4.692	-24.161	-1.260	3.416	1.927	5.094	2.452	1.361	-15.862
		S	-0.324	-7.626	-3.205	-3.334	0.471	4.277	3.821	4.746	-1.175

TABLE VIII (CONT)

MONTH/DIRECTION			NNW	NW	WNW	W	WSW	SW	SSW	S	TOTAL
JUL	(SWELL)	N	0.000	-18.274	-12.337	2.083	2.478	2.601	1.013	0.010	-22.425
		S	0.000	-6.121	-8.492	-1.754	1.103	2.371	1.149	0.106	-11.638
	(SEA)	N	-13.183	-61.519	-0.380	1.198	1.218	3.990	2.111	0.790	-65.775
		S	-1.229	-19.649	-1.893	-1.191	0.179	2.560	2.910	1.481	-16.831
AUG	(SWELL)	N	-0.281	-9.257	-19.391	7.055	3.890	0.244	0.034	0.000	-17.706
		S	-0.029	-2.993	-14.528	-6.082	1.463	0.118	0.055	0.000	-21.995
	(SEA)	N	-8.316	-18.232	-0.177	1.639	0.616	1.325	0.294	1.658	-21.192
		S	-0.533	-5.276	-1.120	-1.623	0.000	1.020	0.820	1.742	-4.970
SEP	(SWELL)	N	-5.158	-1.426	-30.679	10.631	0.428	4.747	0.000	0.946	-20.512
		S	-0.801	-0.465	-18.626	-8.869	0.231	3.347	0.000	1.032	-24.150
	(SEA)	N	-8.442	-11.464	-3.457	-2.193	0.637	2.428	12.414	6.453	0.762
		S	-0.620	-3.331	-4.592	-2.050	0.080	1.666	14.714	14.219	20.086
OCT	(SWELL)	N	0.000	-13.858	-48.527	12.080	6.996	10.786	3.042	4.053	-25.428
		S	0.000	-4.598	-27.906	-10.373	3.527	8.313	1.272	3.052	-26.714
	(SEA)	N	-3.870	-18.474	-1.448	3.410	6.291	33.716	14.776	13.294	47.696
		S	-0.303	-6.076	-2.737	-3.232	1.432	24.648	18.241	18.942	50.915
NOV	(SWELL)	N	-0.560	-10.754	-69.045	16.916	6.156	1.059	3.009	1.683	-50.797
		S	-0.038	-3.396	-42.607	-21.853	3.244	0.971	3.323	1.551	-58.461
	(SEA)	N	-0.714	-15.377	-4.438	2.546	11.529	11.483	21.494	13.110	39.631
		S	-0.043	-5.009	-4.838	-2.405	4.569	8.153	26.201	17.557	44.185
DEC	(SWELL)	N	0.000	-4.584	-36.408	26.228	21.749	9.885	7.102	7.147	31.119
		S	0.000	-1.494	-22.303	-21.121	11.720	9.111	7.916	5.420	-10.751
	(SEA)	N	0.000	-5.867	-10.746	9.328	18.047	28.363	44.683	37.099	12.091
		S	0.000	-0.961	-10.847	-8.435	6.618	23.322	52.311	37.457	99.465
YEAR	(SWELL)	N	-0.394	-8.405	-28.911	14.064	11.244	6.450	6.393	2.519	3.021
		S	-0.064	-2.800	-18.055	-11.682	5.734	5.239	6.181	2.489	-12.930
	(SEA)	N	-5.460	-6.722	-4.937	3.826	5.999	13.041	16.292	15.189	39.997
		S	-0.479	-6.905	-5.246	-3.554	1.933	9.889	18.896	19.496	37.450

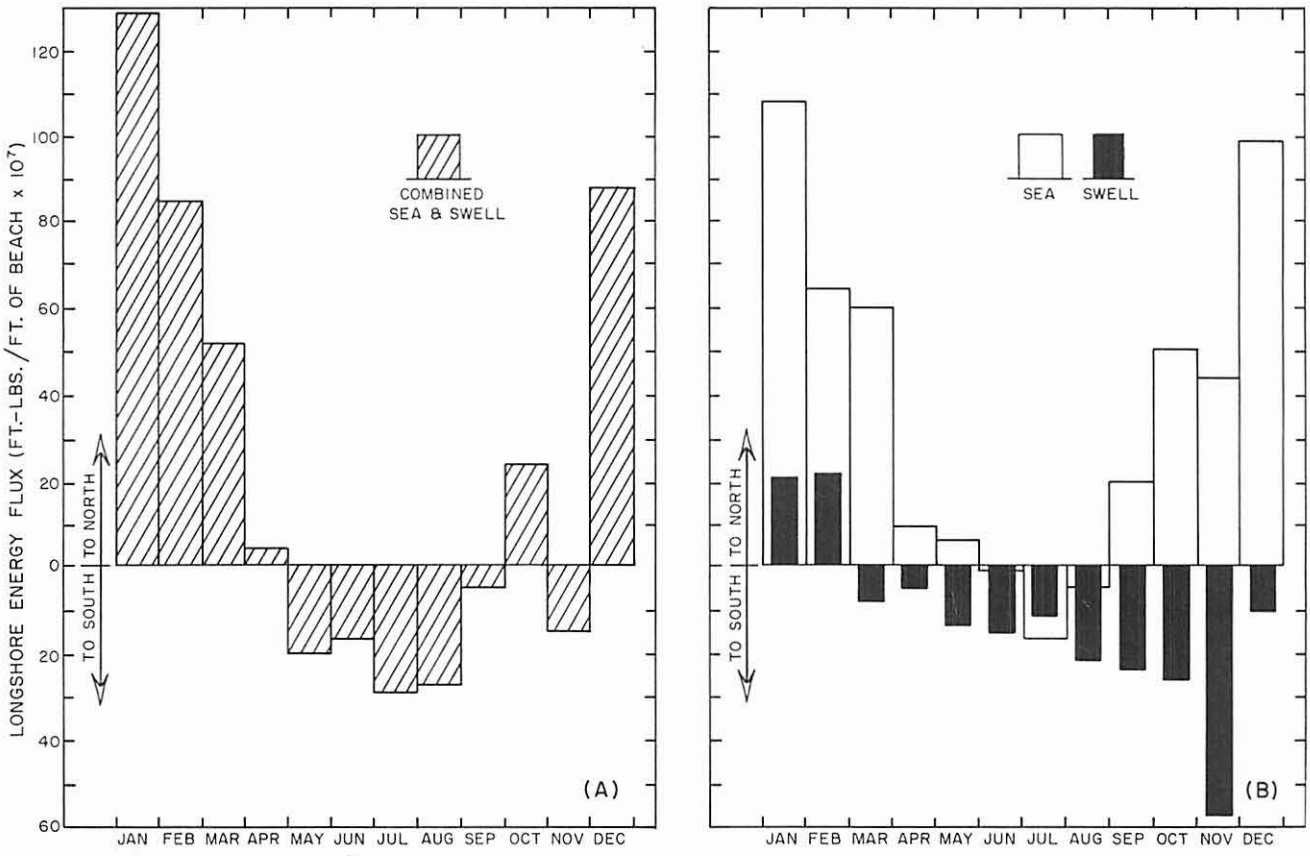

Fig. 17: Relative magnitude and direction of longshore energy flux south of the Columbia River (Station 3).

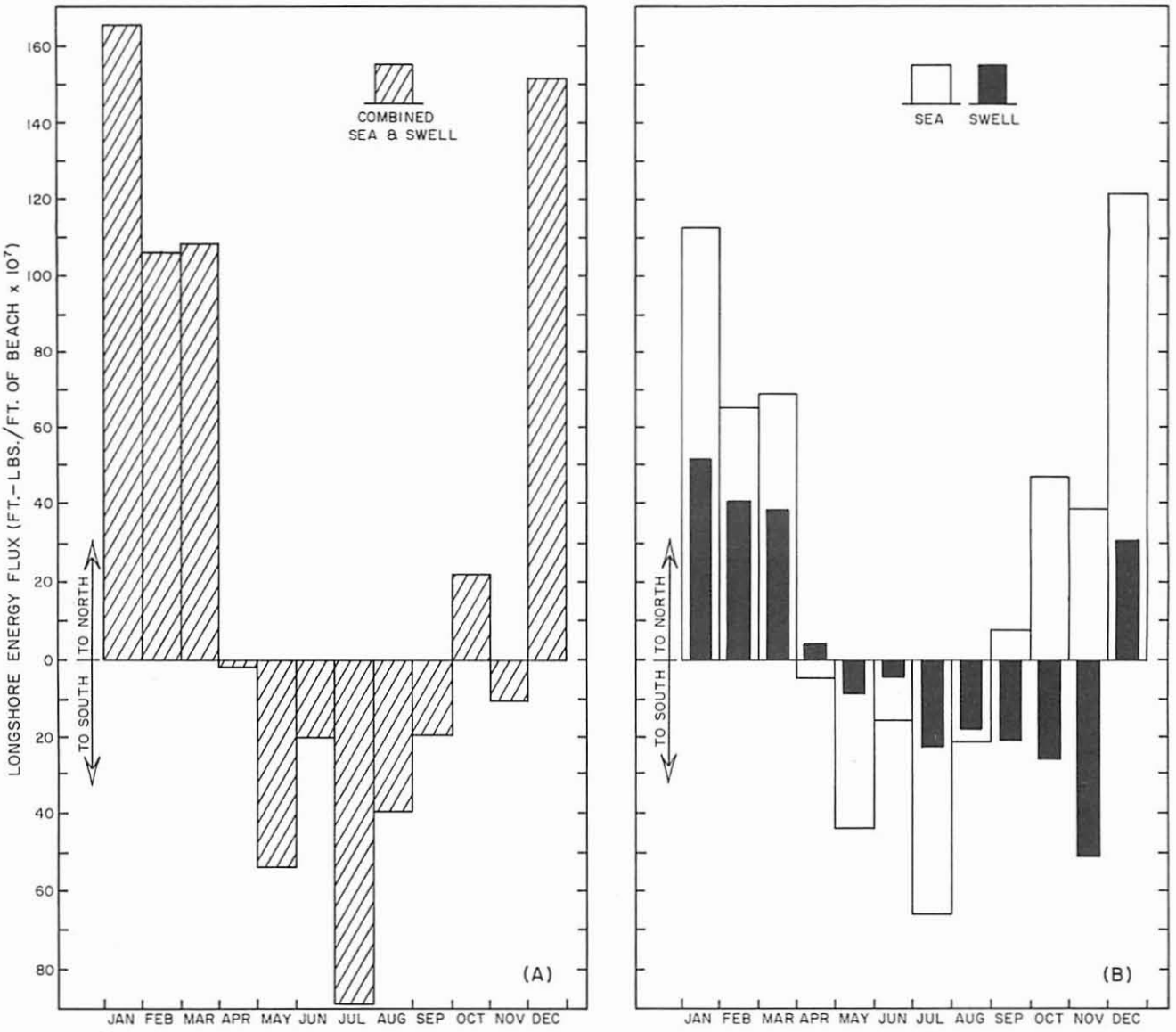

Fig. 18: Relative magnitude and direction of longshore energy flux north of the Columbia River (Station 14).

different picture is gained. For the point south (Station 3) of the Columbia River (Figure 17b), the predominant direction of longshore energy flux is to the south for swell conditions, but with a strong component to the north caused by the seas. The net direction of energy flux for the north station (Station 14) is somewhat similar (Figure 18b). When considering only the swells, a near-balance of longshore wave energy flux results. However, a strong northerly direction of wave energy flux is observed as a result of seas.

Annual conditions of longshore wave energy flux were plotted for both sea and swell directions at points north and south of the Columbia River (Figure 19, Table VIII). The deep-water waves from a westerly direction cause a northerly longshore component of energy flux at Station 14, north of the Columbia River, and to the south at Station 3, south of the Columbia River.

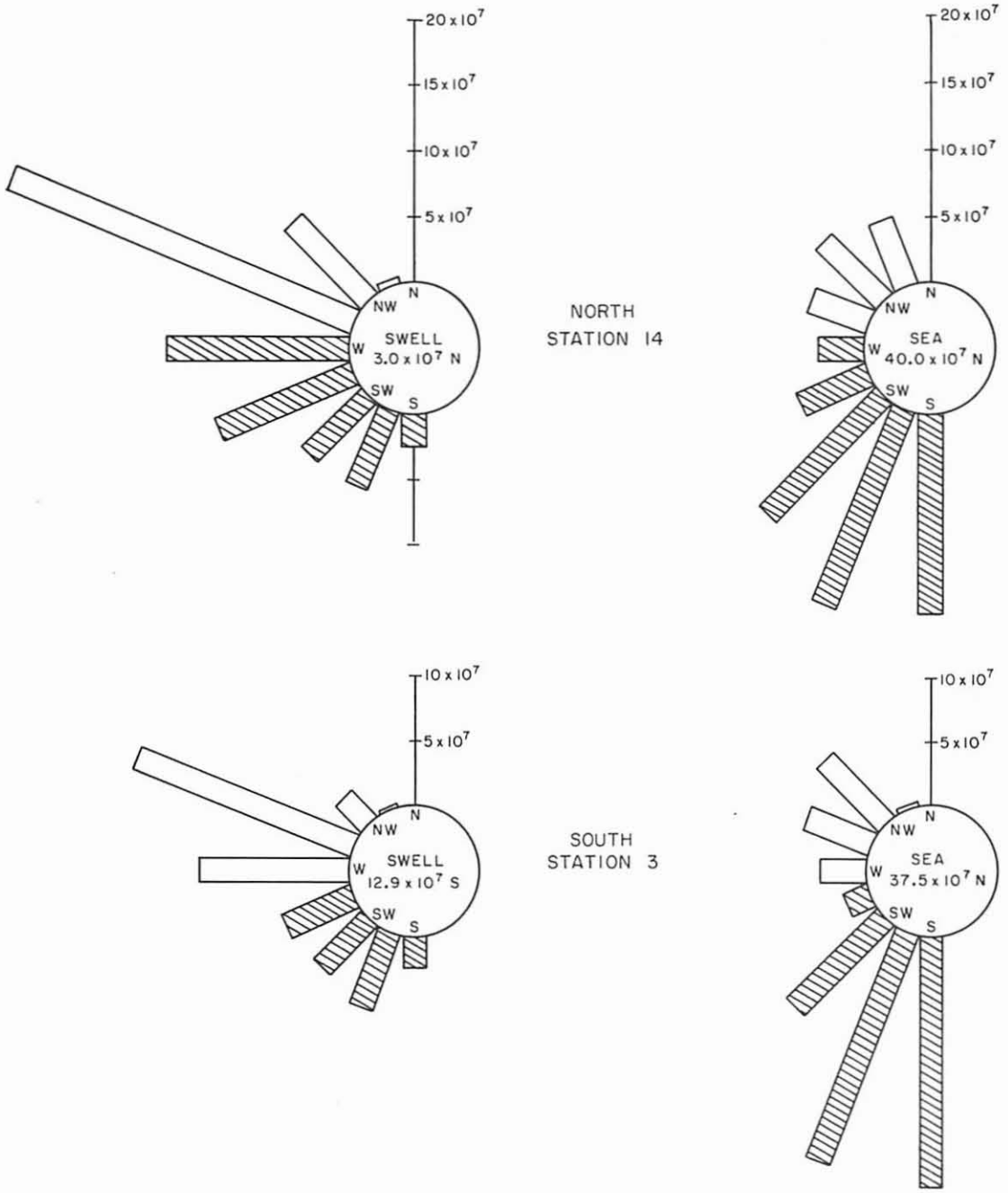

Fig. 19: Energy diagram representing average annual longshore component of wave energy flux in ft.lbs./foot of beach. Ray bearings represent the direction of deep-water wave approach and the length represents the magnitude of the resulting longshore energy flux. Shaded bars represent energy flux to the north and light bars represent southerly energy flux. Net magnitude and direction of energy flux is shown in the center of each energy rose.

DISCUSSION AND INTERPRETATION

Source of Sediments

A natural beach is in dynamic equilibrium when, with a balance between sand supply and erosion, the amount of material entering the area is balanced by the amount being removed. When this balance is disturbed, erosion or deposition takes place. Sediment supply apparently exceeds losses in the study area, resulting in a prograding beach. The rest of the Washington-Oregon coast is apparently eroding, with a retrograding shoreline (Cooper, 1958).

Sediment on a prograding beach is derived from a number of sources that may be grouped under continental land masses, coastal headlands, or offshore zones. The offshore zone has been considered a sediment source considering the onshore transport by shoaling waves (Scott, 1954; Eagleson, Dean, and Peralta, 1957; Nagata, 1962). However, most of the Washington-Oregon coast is eroding, which suggests that, if sediment is being brought inshore by wave action, it is being removed at a greater rate. Assuming that wave action in the study area is similar to that along the coast on either side, the offshore zone is probably unimportant as a source of sediment.

Coastal erosion of headlands no doubt accounts for some of the sediment observed on the beach. Cooper (1958) and Dicken (1961) provide ample evidence of erosion of many of the coastal cliffs of Oregon. The northern Washington coast also shows evidence of rapid erosion. Littoral drift and longshore currents provide a mechanism for moving sediment after it is brought to the beach zone. Wave analyses described earlier indicate a predominant energy flux to the north due to waves in the study area. Trask (1955) demonstrated that some sediment can be moved around promontories even

though they extend into deep water. For this reason, Tillamook Head is probably not a total barrier to sediment movement. However, it is likely to reduce sediment transport into the study area from a southerly direction.

Evidence of coastal erosion is lacking in most of the study area. Beach ridges extend from the seashore to the embayments of Grays Harbor and Willapa Bay (Figure 6). The remainder of the study area has a beach ridge complex that extends inland for at least 0.5 mile (0.8 kilometer) to upland areas, except at North Head, Washington and Tillamook Head, Oregon. These promontories are composed of igneous material, resistant to erosion, and supply very little sediment to the area. Almost all of the highland areas behind the beach ridges support a dense growth of vegetation, further limiting them as sources of sediment.

Sediment from land masses is transported primarily by wind and rivers. The environmental conditions existing in the study area probably limit wind effects to moving sediment inland from the beach after being brought there by other means. Local winds blow in an offshore direction primarily in the winter months, when rainfall and dense vegetation limit the availability of sediment for wind transport (Cooper, 1958). Sand dunes are oriented parallel to the shoreline in the study area and are invading wooded areas (Cooper, 1958), supporting the view that the predominant wind effect is onshore.

River outflow is the most probable mechanism of sediment addition to the beach. The association of sand dunes with all major stream outlets supports this view. The Columbia River is by far the largest river in the area and its adjoining sand dune complex is also the largest.

Heavy mineral analyses suggest that the Columbia River is a major contributor of sediment. The analyses were performed only on the 3.0 to 3.5

phi grain-size range for each sample. According to Rubey (1933) the best method of studying heavy minerals without excessive laboratory work was to select two size-ranges, one that was the same for all samples and one that would vary with a given parameter such as the mean grain-size. On this basis, the 3.0 to 3.5 phi size was selected. Due to the good sorting exhibited by the sediment, more than 90 percent of the samples at each typical depth had a mean grain-size that remained constant within a given size range (Figure 9). Within these limits it was assumed that one grain-size range would represent both the constant size and relative size criteria described by Rubey, and would be representative of the entire sample.

The high percentage of heavy minerals in the vicinity of the Columbia River rapidly decreases in both directions along the coast (Figure 13). Grays Harbor is the only place in the study area that has heavy mineral frequencies approaching those of the Columbia River. A much smaller increase is observed around Willapa Bay. These increases may be due to addition from a nearby source or as a result of preferential transport of certain minerals, as transport is controlled by the size, shape, and density of a mineral (Pettijohn, 1957, ch. 12).

The relative proportions of magnetic minerals imply that the drainage basin associated with the Columbia River is a primary sediment source (Figure 13). No significant increase of magnetic constituents is observed near the mouth of Willapa Bay, though the total heavy mineral content does increase. Only a minor increase in magnetic constituents is observed at Grays Harbor. This implies that neither Willapa Bay nor Grays Harbor are major contributors of magnetic minerals, of the size range studied, to the nearby beaches. The increase in heavy minerals at Willapa Bay may be explained by the greater energy expended at spits due to wave refraction and

convergence (Kuenen, 1950, p. 81) as well as high current velocities due to tidal influences.

The rapid increase of heavy minerals immediately north of Grays Harbor is probably due to addition from another source. Sediment may be added either from inside the harbor or from jetty breakdown. High berms on both sides of the entrance are composed almost entirely of basalt pebbles. This material is no doubt derived from the jetties, which are composed of basalt. Waves are very active in jetty breakdown, and the jetties at Grays Harbor have been repaired several times (U.S. Army Corps of Engineers, 1962). Further breakdown of the gravel may result in an increase in heavy minerals.

The results of individual heavy mineral frequencies (Figure 14) give further evidence supporting a river source of sediment. Hypersthene occurs in some abundance around the Columbia River and Willapa Bay. Pettijohn (1957) determined the "order of persistence" of common rock-forming minerals and found that hypersthene has a very low resistance to solution. It is rare in sediments pre-dating the Pleistocene.

Hypersthene may be unstable on the beaches as a great deal of solution pitting is observed on the crystals. The abundance of hypersthene decreases rapidly with distance from the entrances, as demonstrated by frequency counts and hypersthene/hornblende ratios (Figure 15). However, euhedral crystals are commonly observed both in the immediate vicinity of Willapa Bay and especially at the Columbia River.

Waters (1962) described the volcanic rock types of the Northwest Pacific area of the United States by means of their heavy mineral content and describes hypersthene as the characteristic mineral associated with andesite flows and associated pyroclastic deposits of the Cascade Range. The relationship of the flows to regional drainage (Figure 3) suggests that

the Willamette River may be the major contributor of hypersthene to the Columbia River. Dams located on the Columbia River probably trap much of the coarse sediment associated with this river. However, the Willamette River carries a very large sediment load (Fenneman, 1931) and empties into the Columbia River below the dams.

The predominance of hypersthene over other heavy minerals in the vicinity of the Columbia River is a qualitative measure of the importance of the river as a source of sediment. The local increase of hypersthene near the north end of the Willapa Bay entrance may be the result of active erosion that has removed a portion of the spit off Cape Shoalwater in the last 75 years. A south-trending spit occupied the area of the present main channel at Willapa Bay, but recent erosion has removed approximately 2.1 miles (3.4 kilometers) of the spit. This erosion may have resulted in a residual deposit of hypersthene to account for its observed increase. Reworking of sediment is implied by this process rather than addition to the beach. However, Willapa Bay may also be a minor contributor of sediment from a landward source as some euhedral hypersthene crystals are found at the entrance. Contributions of this nature are probably small because the bay is essentially a tidal flat with only small streams draining into it.

Another possible source of sediment is related to the drainage in the vicinity of Grays Harbor. The Chehalis River Valley is a glacial outwash channel formed during the retreat of the last ice sheet (Campbell, 1962). During the period of lowered sea level associated with the ice age, the Chehalis River probably extended to or beyond the present harbor entrance. Coarse material associated with the glacial outwash may have remained as a residual deposit and may account for some of the pebbles and cobbles of sedimentary and intrusive igneous rocks. Jetty material appears to be

composed entirely of basalt, eliminating it as a source of these particular pebbles. However, the pebbles and cobbles do not make up an important part of the coarse material and appear to be of little importance as a contributor of sediment to the beach.

The recent bathymetric changes near the mouth of the Columbia River (Figures 4 and 5) suggest only limited sediment influx from coastal erosion. The south jetty of the Columbia River was constructed during the period 1885-1895 (Lockett, 1962). Apparently the broad shoal areas, associated with the mouth of the river, were affected by the jetty. The large amounts of sediment that were brought by the river to the river mouth were originally dispersed both to the north and south by variable wave attack (Figures 17 and 18). The south jetty blocked sediment movement to the south and apparently extended into water of such depth that wave action was not capable of moving sediment at these depths. Thus, the jetty acted as a barrier to southward movement of river-derived sediment.

If northward-moving sediment of the winter months could bypass Tillamook Head in sufficient quantity, the shoal area could have been maintained, but this apparently does not occur. This indicates that sediment associated with erosion of the Oregon coast is of limited importance as a source of sediment being supplied to the study area.

Direction of Sediment Movement

The direction of sediment movement in the beach zone is primarily determined by the predominant direction of wave attack. Movement of water over the bottom exerts a tractive force on sediments, and when this force exceeds the particle's resistance to movement, transport occurs (Johnson, 1956). The net movement of sediment in the zone offshore from the breaker

zone is almost always shoreward (Ippen and Eagleson, 1955; King, 1959). In this zone, the volume transport of sediment increases with an increase of wave period, energy, and with decreasing depth. As a wave moves into shallow water the crest peaks and the trough appears to lengthen and become flatter. The horizontal components of water particle orbital velocities are equal under the trough and crest in deep water, but the shoreward velocity component becomes greater in the shoaling wave (King, 1959).

Wave length appears to be an important factor in the direction of sediment movement seaward of the breaker zone. A wave is affected by bottom topography at a depth of approximately 1/2 the wave length. Wave refraction causes wave crests to tend to become oriented parallel to the shoreline, and longer waves have a greater distance in which to become so oriented. Thus, due to wave refraction, the migration of sediment associated with longer waves (e.g., swells) tends to be directly shoreward rather than the original deep-water wave direction.

Nagata (1962) measured suspended sediment load in a cross-section through breaker zones under natural conditions and found that the greatest concentration of suspended sediments occurred just inside the break-point and decreased rapidly in an offshore direction. Mason (1953) stated that as much as 80 percent of sediment moved by wave action was moved inside the break-point. It is generally assumed that longshore currents are set up as a result of waves breaking at an angle to the shoreline. The velocity of the longshore currents definitely increases with an increase in wave steepness (Saville, 1950; Arlman, Santema, and Svasek, 1958). It would appear that wave steepness would be an important factor in sediment movement inside the breaker zone.

Saville's (1950) model studies of sediment transport related to wave steepness were considered when grouping the steepness values (Table VII). He reported that maximum sediment transport occurred at beaches in equilibrium with wave attack when steepness values ranging from 0.015 to 0.025 were present. Values above and below this range resulted in greatly reduced sediment movement.

Assuming that model studies are applicable to natural beaches, the following conditions are found in the study area. Locally-formed waves (seas) with steepness values in the range 0.015 to 0.025 occur more than 90 percent of the time. However, swells of the same steepness values occur less than 20 percent of the time (Figure 16). They generally have steepness values that are less than 0.015. The predominance of "seas" over swells for the range 0.015 to 0.025 is evident. These results suggest that "seas" are the major factor involved in sediment movement in the study area. However, the net direction of sediment movement is still difficult to determine. The frequencies with which both seas and swells arrive at the study area from various directions are such that a near balance of net direction is obtained (inset, Figure 16). This condition would result in an apparent local movement of sediment back and forth with seasonal changes in direction.

Utilizing the same wave data, a clearer picture of the wave conditions in the study area was obtained by considering wave energy flux. When working with wave steepness ratios, the seasonal effect of larger winter waves was not obvious because waves of different heights may have the same steepness ratios if their lengths varied by a proportionate amount.

When determining the longshore component of wave energy flux, seasonal variations became more obvious. The winter wave regime (December-March) resulted in strong longshore energy flux to the north at points both north

(Station 14) and south (Station 3) of the Columbia River (Figures 17a and 18a). The smaller summer energy flux was directed to the south, reflecting the seasonal wind shift and more moderate wave conditions typical of the Northeast Pacific.

When plotting the energy flux values for sea and swell individually, the relative effects of each are obvious (Figures 17b and 18b). Longshore energy flux due to seas is predominant to the north for most of the year at both points studied. Energy flux due to swells nearly balances north of the Columbia River, and has a net southerly component south of the Columbia River. However, the magnitude of energy flux is much smaller for swell than sea in both cases, as the greater average wave lengths associated with swells cause wave refraction to occur over a greater distance resulting in crests that are more nearly parallel to the shoreline when breaking. The smaller angle of incidence causes a correspondingly lower value in the longshore component of wave energy flux. These observations support the findings of wave steepness considerations, which gave more importance to seas than swells for sediment movement. The southerly direction of energy flux at Station 3 is no doubt due to the orientation of the beach in relation to the average direction of wave attack.

The results of average annual longshore energy flux (Figure 19) support the monthly data and point out one important difference between points north and south of the Columbia River. Longshore energy flux as a result of waves from due west results in a northerly energy flux north of the river and a southerly energy flux south of the river. This is important when considering swell data, as the greatest percentage of swells arrive from the west. However, the opposite directions of energy flux due to swells are dominated by the net energy flux to the north due to seas.

Clatsop Beach has the smallest average grain size (2.65 phi) in the study area (Table II). The construction of the south jetty of the Columbia River apparently limited sediment movement from the river in a southerly direction. Probably only smaller sizes are capable of movement around the jetty. Tillamook Head is another obstruction to sediment movement from the south, again allowing only finer sediment to migrate around the promontory.

The sediments of Clatsop Beach showed a slight seasonal shift to coarser sizes in the winter. Wave refraction and divergence of wave orthogonals is reduced in the winter because the beach is oriented such that wave crests approach nearly parallel to the shoreline. Winter waves are larger and more capable of removing fine sediment. These conditions probably account for the observed change in mean size.

The sediments of Clatsop Beach are well-sorted, as are the sediments of most of the study area (Figure 10). Sorting appears to improve slightly during winter conditions (Table III). Skewness values are relatively small, and approach zero in the winter months. The beach sediments closely approach a log-normal distribution, especially in the winter.

Clatsop Beach appears to be an isolated beach with only limited sediment influx. Most of the observed changes (Figure 2) occurred soon after jetty construction, and the beach presently maintains an equilibrium profile (O'Brien, 1951). Seasonal changes in sediment characteristics are primarily due to wave action. Good sorting and low skewness values result from wave action on sediment that receives only a small amount of new material.

Long Beach sediments have a grand mean size that is consistent at 2.48 phi summer and winter. This is nearly the same as the average grain size for the Columbia River samples (2.50 phi). The similarity of average sizes implies that sediment may move from the Columbia River to this zone.

Inman (1949) found that the most easily moved sediment was one with a mean size of 0.18 mm. This may be expressed in phi values as a range from 2.44 to 2.51 phi (0.184 to 0.175 millimeters). Long Beach and Columbia River sediments fall in this size range (Table II).

The seasonal shift in mean size at the 20-foot and 30-foot depths of Long Beach are toward slightly finer sediment in the winter (Figure 9), which is the reverse of Clatsop Beach. Sediments probably migrate to Long Beach in the winter from the Columbia River entrance area. Wave analyses (Figures 17 and 18) show that wave energy flux is to the north during the winter months. Long-period waves associated with storms cause sediment movement at greater depths during this season.

Long Beach sediments are better sorted than in the other beach zones. Inman (1949) concluded that because sediment of 0.18 millimeter size was the most easily transported, it should also have the best sorting. Seasonal changes in sorting are opposite to those of Clatsop Beach; sorting is poorer in the winter than in the summer. An influx of finer sediment would result in a greater range of sediment sizes and poorer sorting coefficients. The size distribution of beach sediments also becomes more skewed in the winter (Table IV). This condition would result from an influx of sediment of a different mean size.

Long Beach apparently receives sediment during the winter months from the Columbia River. It is composed of sediment of the most easily moved size range. The Columbia River entrance contains sediment of approximately the same mean size. The period of maximum run-off is generally during April and May (Lockett, 1962), and is probably the period of greatest sediment deposition in the zone offshore from the estuary. However, summer is also the period of smaller waves and southerly component of wave energy flux.

Waves are probably not of sufficient magnitude to move sediment beyond deep water adjacent to the south jetty and onto Clatsop Beach. The seasonal shift to winter conditions, with larger waves and energy flux to the north, results in sediment migration to Long Beach.

Twin Harbors Beach reflects a greater variation in sediment sizes than the other beaches. The sediment of the portion of the beach adjoining Grays Harbor undergoes large seasonal changes in mean size. During the summer the sediment is much coarser than during the winter. The direction of longshore energy flux (Figures 17 and 18) can probably explain these seasonal changes. The Grays Harbor area apparently has a residual sediment deposit of gravel that is alternately exposed and covered seasonally. The northerly movement of fine sediment in the winter covers the coarse sediment south of Grays Harbor. The residual coarse sediment is again exposed in the summer, when south-setting littoral transport removes the fine sediment. Jetties block movement of fine sediment into this area from the north. The same sequence would probably occur at the Columbia River except for sediment addition from the river, which could effectively mask gravel deposits from jetty breakdown.

Sorting is poor in the summer near the Grays Harbor entrance. Removal of much of the fine sediment by littoral drift results in a greater proportion of coarse sediment (Figure 8). The deviation of the sorting coefficients is also quite large (Table III). Winter conditions allow an influx of finer-grained sediment that is well-sorted. This sediment appears to mask the coarser sediment observed in summer conditions.

Twin Harbors Beach sediment also becomes more skewed in the winter, and in a negative direction. This is due to the relatively large change of mean size to the fine sizes. A condition similar to that of Long Beach

occurs, but the slight change of mean size in Long Beach results in a greater skewness shift in the positive direction, because sorting gets poorer.

The mean size varies only slightly across Willapa Bay (Figure 8). This is contrary to conditions at both the Columbia River and Grays Harbor. This observation supports the results of heavy mineral and magnetic mineral analyses in suggesting that the drainage system associated with Willapa Bay does not contribute significant amounts of sediment to the beach.

Heavy mineral results support the evidence gained from mechanical and wave energy analyses. The greatest concentration of heavy minerals of the 3.0 to 3.5 phi size range is immediately north of the Columbia River. The Willapa Bay area shows a moderate increase of heavy minerals, but no observable sediment movement. The increase may be due only to the greater energy expenditure of tidal currents and waves at the bay entrance selectively removing the lighter constituents.

Magnetic minerals show no increase in frequency across the Willapa Bay entrance (Figure 13). However, a definite increase in the relative proportions of magnetic minerals is observed at the Columbia River. The absence of variations across Willapa Bay further supports the view that the bay does not supply sediment to the beach in significant amounts. The greatest frequency of magnetic constituents is immediately north of the Columbia River. A slight increase is also observed just north of Grays Harbor. These data provide further evidence that the primary direction of sediment movement is to the north. Sediment can apparently bypass Willapa Bay. The entire entrance is quite shallow and breakers can be observed over much of this area.

Individual mineral counts (Figure 14) provide additional clues as to

net sediment movement. Hornblende appears throughout the study area in fairly constant amounts. Pettijohn (1957) shows that hornblende is one of the common rock-forming minerals that is quite resistant to weathering. It was used as a base for computing frequency ratios. Hypersthene/hornblende ratios reach a maximum north of the Columbia River. Assuming the river to be a source of hypersthene, its increase in frequency to the north of the river is an indication of net direction of movement. A similar increase in ratio is observed north of Willapa Bay, suggesting that it may also supply sediment to the beach. However, it may also be due to the extensive erosion of Cape Shoalwater, as discussed earlier.

Further evidence of net direction of sediment movement is provided by bathymetric changes in the study area (Figures 4 and 5). The most important changes are the loss of sediment immediately south of the south jetty (Figure 1), and the gain, in the form of a crescent-shaped bar, offshore and to the north of the estuary. Figure 5 shows a continued outbuilding of the offshore bar immediately beyond the earlier bar. The apparent north-trending movement of the bars implies a northerly net sediment movement. The loss of sediment south of the south jetty suggests that wave action has continued to move sediment onshore in this zone while the south jetty has essentially blocked southward movement of sediment from the river to replenish the area. The second chart shows that the area south of the south jetty has apparently reached an equilibrium profile with little change since 1926.

Channel changes have been observed in the Columbia River that imply sediment movement to the north. A chart by Admiral Vancouver in 1792 (Lockett, 1962) shows a single channel for the Columbia River. Two channels are observed in a chart made in 1839, resulting from a breakthrough at Clatsop Spit. By 1885, the river had returned to a single channel because

the island that had broken off from Clatsop Spit had migrated to the position now held by Sand Island. These changes suggest a northward movement of sediment. The accumulation of sediment north of Clatsop Spit appears to divert the current to the north side of the estuary. The north jetty is presently being actively undercut by river currents while the south jetty is protected by large sand deposits (Lockett, 1962).

The changes of the Clatsop Beach shoreline subsequent to jetty construction are presented in Figure 2. An immediate build-up of sediment occurred to form Clatsop Spit, and continued until sand breached the jetty as shown in the diagram (Dicken, 1961). The major cause of this phenomenon is probably wind, after wave action brought the sediment to the beach from offshore.

A similar occurrence appears to be happening at Willapa Bay. Sand migrating to the north has deflected the channel currents to cause erosion of Cape Shoalwater. In 1962 a new channel broke through the outer bar several miles north of the old channel. A smaller channel is observed at Leadbetter Point, at the south end of the Willapa Bay entrance. It is conceivable that the isolated sand island will continue to migrate to the north side, at which time a single channel may be formed south of the migrating island.

PROPOSED ANNUAL SEQUENCE OF EVENTS

The wave regime in the vicinity of the Columbia River entrance has a definite seasonal character. During the summer, waves are predominantly from the northwest causing longshore currents directed to the south. During the winter the directions reverse. Winter storm conditions probably cause more sediment transport than do summer conditions.

The sediment deposited in a crescent-shaped bar immediately offshore from the Columbia River jetties is probably derived primarily from the Columbia River. Maximum run-off occurs during May and June, at which time the river is most capable of depositing sediment outside the estuary.

Waves and associated littoral currents of summer tend to move sediment in a southerly direction. These waves are apparently not capable of moving significant quantities of sediment south past the Columbia River jetties. Sediment can probably move past Willapa Bay in either direction. The estuary and jetties of Grays Harbor are probably more effective in blocking sediment movement.

During the winter, long-period waves associated with storms are probably capable of moving sediment shoreward from the offshore zones at the Columbia River and Grays Harbor. Associated littoral transport moves sediment to the north. Fine-grained sand moves into the Grays Harbor area, concealing the coarse material left as a residual deposit during summer. Some sediment is probably added to the beaches from coastal erosion below Tillamook Head. The greater wave energy of winter conditions results in a net northerly migration of sediment.

CONCLUSIONS

Beaches in the vicinity of the Columbia River receive material from two major sources, the sediment load associated with river outflow and longshore transport of material from coastal erosion. The Columbia River is the dominant supplier and probably accounts for the prograding beaches that characterize the study area. It apparently deposits sediment in a crescent-shaped bar immediately offshore and to the north of its jetties.

The drainage system associated with Willapa Bay probably does not contribute an appreciable amount of new sediment to the beaches. Erosion and reworking results in sediment modification at the entrance area. New sediment is added to the beaches near Grays Harbor, primarily as a result of jetty breakdown. Possibly glacial outwash from the Chehalis River Valley contributed some coarse material that has remained behind. This would account for gravel in the immediate area that cannot be related to jetty breakdown.

Longshore movement of material resulting from coastal erosion probably has some influence on the sediment budget. However, free movement of sediment in the study area is inhibited by obstructions such as promontories, estuaries, and jetties.

The net direction of sediment movement is in a northerly direction. Wave analyses reflect a net northerly direction of wave energy flux which is predominant in the winter months. Storms occur most frequently in the winter and usually approach the coast from a southwest direction. Long-period waves associated with storms are capable of moving sediment shoreward from relatively deep water to a point where littoral drift can redistribute the sediment alongshore.

The northerly net movement of sediment is further implied by the results of mechanical and heavy mineral analyses of the beach sediment. The mean grain-size of Long Beach sediment is similar to that of sediment at the entrance of the Columbia River. Sediment movement south to Clatsop Beach is prohibited by the south jetty. Loss of sediment in the nearshore zone immediately south of the Columbia River jetties has occurred since their construction. A significantly smaller mean grain size is found at Clatsop Beach than the rest of the study area.

The maximum relative frequency of heavy minerals in the beach sediment occurs immediately to the north of each entrance area. Hypersthene is almost certainly from river sources, and it also reaches a maximum at the same locations, particularly at the Columbia River.

Evidence of a general northward sediment movement is available from several events that have been observed at the entrance areas. The migration of Sand Island from Clatsop Beach to the north side of the Columbia River has been traced on navigation charts. The main channels of the Columbia River and Willapa Bay are apparently in the process of migrating to the north due to sediment deposition at the southern edges of the entrance areas.

Seasonal changes in the direction of wind and wave attacks on the coast cause reversals in the direction of sediment movement. The orientation of the coastline further north may be such that wave energy flux becomes dominant to the south in that area. The south-trending spit at Grays Harbor suggests that movement to the south may be of more importance in this region. However, the results of this study provide evidence of a net northerly direction of beach sediment transport in the vicinity of the Columbia River.

REFERENCES

Arlmann, J. J., P. Santema, and J. N. Svasek, 1958. "Movement of bottom sediment in coastal waters by currents and waves." Beach Erosion Board, Tech. Memo., 105. 55 pp.

Arnold, R., 1906. "Geological reconnaissance of the coast of the Olympic Peninsula, Washington." Bull. Geol. Soc. Am., 17:451-468.

Baldwin, E. M., 1959. Geology of Oregon. Ann Arbor, Michigan: Edwards Bros. 125 pp.

Barnes, C. A., and R. G. Paquette, 1957. "Circulation near the Washington coast." Proc. 8th Pacific Sci. Congr., 3:585-606.

Bruun, P., 1963. "Longshore currents and longshore troughs." J. Geophys. Res., 68:1065-1077.

Caldwell, J. M., 1956. "Wave action and sand movement near Anaheim Bay, California." Beach Erosion Board, Tech. Memo., 68. 21 pp.

Campbell, C. D., 1962. Introduction to Washington Geology and Resources. Wash. Div. Mines and Geol., Olympia, Washington. 44 pp.

Cooper, W. S., 1958. "Coastal sand dunes of Oregon and Washington." Geol. Soc. Am., Memoir, 72. 169 pp.

_____, 1959. "Sand dune development and sea-level changes on the coast of North Oregon." Bull. Geol. Soc. Am., 65:1373.

Creager, J. S., D. A. McManus, and E. E. Collias, 1962. "Electronic data processing in sedimentary size analyses." J. Sediment. Petrol. 32:833-839.

Dicken, S. N., 1961. Some recent changes of the Oregon coast. Dept. of Geog., Univ. of Oregon, Eugene, Oregon. 150 pp.

Eagleson, P. S., R. G. Dean, and L. A. Peralta, 1957. "The mechanics of the motion of discrete spherical bottom sediment particles due to shoaling waves." Mass. Inst. of Tech. Hydrodynamics Lab., Cambridge, Mass., Rept., 26. 40 pp.

Eagleson, P. S., and J. W. Johnson, 1960. Coastal Processes, from Estuary and Coastline Hydrodynamics (course no. 1.67 s.). Unpubl. papers, Hydrodynamics Lab., Mass. Inst. Tech., Cambridge, Mass.

Fenneman, N. M., 1931. Physiography of Western United States. New York: McGraw Hill. 534 pp.

Fessenden, F. W., 1959. "Removal of heavy liquid separates from glass centrifuge tubes." J. Sediment. Petrol., 29:621.

Folk, R. L., and W. C. Ward, 1957. "Measures for describing size of sediments whose size frequency curves are non-normal." J. Sediment. Petrol., 27:3-26.

Glover, S. L., 1940. "Pleistocene deformation in the Olympic coastal region." Northwest Sci., 14:69-71.

Griggs, A. B., 1945. "Chromite-bearing sands of the southern coast of Oregon." U.S. Geol. Surv., Bull., 945e:113-150.

Handin, J. W., and J. C. Ludwick, 1950. "Accretion of beach sand behind a detached breakwater." Beach Erosion Board, Tech. Memo., 16. 15 pp.

Herrin, E., H. S. Hicks, and H. Robertson, 1958. "A rapid volumetric analysis for carbonate rocks." Field and Lab., 26:139-144.

Hodge, E. T., 1938. "Geology of the Lower Columbia River." Bull. Geol. Soc. Am., 49:831-930.

Honar, R. R., 1918. "Notes on the black sand deposits of Southern Oregon and Northern California." U.S. Dept. Interior, Bur. Mines, Tech. Paper, 196. 42 pp.

Hundhausen, R. J., 1947. "Chromiferous sand deposits in Coos Bay area, Cass County, Oregon." U.S. Bureau of Mines, Rept., 4001. 13 pp.

Inman, D. L., 1949. "Sorting of sediments in the light of fluid mechanics." J. Sediment. Petrol., 19:51-71.

_____, 1952. "Measures for describing size of sediments." J. Sediment. Petrol., 22:125-145.

Ippen, A. T., and P. S. Eagleson, 1955. "A study of sediment sorting by waves shoaling on a plane beach." Beach Erosion Board, Tech. Memo., 63. 80 pp.

Johnson, J. W., 1956. "Dynamics of nearshore sediment movement." Am. Assoc. Petrol. Geologists, 40:2211-2231.

King, C. A. M., 1959. Beaches and Coasts. E. Arnold Ltd., London, 390 pp.

Krumbein, W. C., and F. J. Pettijohn, 1938. Manual of Sedimentary Petrography. New York: Appleton-Century-Crofts, Inc. 535 pp.

Krumbein, W. C., and H. A. Slack, 1956. "Relative efficiency of beach sampling methods." Beach Erosion Board, Tech. Memo., 90. 43 pp.

Kuenen, Ph. H., 1950. Marine Geology. New York: John Wiley & Sons. 567 pp.

Lockett, J. B., 1962. Phenomena affecting improvement of the Lower Columbia River. U.S. Army Engineer Div., North Pacific, Portland, Oregon. 42 pp.

Lowry, W. D., and E. M. Baldwin, 1952. "Late Cenozoic geology of the Lower Columbia River Valley, Oregon and Washington." Bull. Geol. Soc. Am., 63:1-24.

Lupton, C. T., 1915. "Oil and gas in the western part of the Olympic Peninsula, Washington." U.S. Geol. Soc., Bull., 581:23-81.

Mason, M. A., 1953. "Surface water wave theories." Trans. Am. Soc. Civil. Engrs., 118:569.

McLaughlin, W. T., T. Willard, and R. L. Brown, 1942. "Controlling coastal sand dunes in the Pacific Northwest." U.S. Dept. Agr., Circular, 660. 46 pp.

Munk, W. H., and M. A. Traylor, 1947. "Refraction of ocean waves; a process linking underwater topography to beach erosion." J. Geol., 55:1-26.

Nagata, Y., 1962. "Balance of the transport of sediment due to wave action in shoaling water, surf zone and foreshore." Records of Oceanographic Works in Japan, 6:53-62.

National Marine Consultants, 1961a. Oceanographic study for Columbia River Entrance. Nat. Marine Consultants, Santa Barbara, California. 16 pp.

_____, 1961b. Wave statistics for three deep-water stations along the Oregon-Washington coast. Nat. Marine Consultants, Santa Barbara, California. 16 pp.

O'Brien, M. P., 1948. Wave action and salinity currents at the mouth of the Columbia River. Fluid Mechanics Lab., Univ. of Calif., Berkeley, Calif. 7 pp.

_____, 1951. "Wave measurements at the Columbia River light vessel, 1933-1936." Trans. Am. Geophys. Union, 32:875-877.

Pardee, J. T., 1929. "Platinum and black sand in Washington." U.S. Geol. Survey, Bull., 805:1-15.

_____, 1934. "Beach placers of the Oregon coast." U.S. Geol. Surv., Circular, 8. 41 pp.

Pettijohn, F. T., 1957. Sedimentary Rocks. New York: Harper & Bros. 715 pp.

Pierson, W. R., G. Neumann, and R. James, 1953. Practical methods for observing and forecasting ocean waves by means of wave spectra and statistics. Research Div., College of Eng., New York Univ., New York. 10 pp.

Putnam, J. A., W. H. Munk, and M. A. Traylor, 1949. "The prediction of longshore currents." Trans. Am. Geophys. Union, 30:337-345.

Rubey, W. W., 1933. "The size distribution of heavy minerals within a water-laid sandstone." J. Sediment. Petrol., 3:3-29.

Saville, T., 1950. "Model study of sand transport along an infinitely long, straight beach." Trans. Am. Geophys. Union, 31:555-565.

Scott, T., 1954. "Sand movement by waves." Beach Erosion Board, Tech. Memo., 48. 16 pp.

Shepard, F. P., 1954. "Nomenclature based on sand-silt-clay ratios." J. Sediment. Petrol., 24:151-158.

Strahler, A. N., 1960. Physical Geography. New York: John Wiley & Sons. 504 pp.

Sverdrup, H. U., M. V. Johnson, and R. H. Fleming, 1942. The Oceans, Their Physics, Chemistry, and Biology. Englewood Cliffs: Prentice-Hall. 1050 pp.

Trask, P. D., 1955. "Movement of sand around Southern California Promontories." Beach Erosion Board, Tech. Memo., 76. 60 pp.

Tully, J. P. and F. G. Barber, 1961. "An Estuarine Model of the Sub-Arctic Pacific Ocean." In: Mary Sears (Editor), Oceanography. Baltimore: Horn-Shafer Co., pp. 425-543.

Twenhofel, W. H., 1943. "Origin of the black sands of the coast of southwest Oregon." Oregon Dept. Geol. and Min. Ind., Bull., 24. 25 pp.

Twenhofel, W. H., 1946a. "Beach and river sands of the coastal region of southwest Oregon with particular reference to beach sands." Am. J. Sci., 244:114-135.

_____, 1946b. "Mineralogical and physical composition of the sands of the Oregon coast from Coos Bay to the mouth of the Columbia River." Oregon Dept. Geol. and Min. Ind., Bull., 30. 64 pp.

U.S. Army Corps of Engineers, 1933. Mouth of the Columbia River, current survey. Engineer District, Portland. 45 pp.

_____, 1938. Mouth of the Columbia River, Oregon and Washington. Engineer District, Portland. 15 pp.

_____, 1951. "Bar and entrance conditions, October, 1949, Grays Harbor." In: Harbor entrance topography. Map file No. E-5-1-44, plate A-10.

_____, 1961. "Shore protection, planning, and design." Beach Erosion Board, Tech. Rept., 4. 242 pp.

_____, 1962. "Study Program of Grays Harbor." U.S. Army Engineer District, Seattle, Washington, 13 pp; 11 plates.

U.S. Tidal Model Lab., 1935. "Mouth of the Columbia River, beach erosion investigations, report on experiments of July, 1933 - May, 1935." U.S. Tidal Model Lab., Berkeley, Calif., Tech. Memo., 7. 60 pp.

_____, 1936. "Mouth of the Columbia River, beach erosion investigations, summary of observations and results." U.S. Tidal Model Lab., Berkeley, Calif., Tech. Memo., 20. 29 pp.

Waters, A. C., 1962. Basalt magma types and their tectonic associations: Pacific Northwest of the United States. Am. Geophys. Union, Monograph, 6:158-169.

Watts, G. M., 1953. "A study of sand movement at South Lake Worth Inlet, Florida." Beach Erosion Board, Tech. Memo., 42. 23 pp.

Wentworth, C. K., 1922. "A scale of grade and class terms for clastic sediments." J. Geol., 30:377-392.

APPENDIX I

DERIVATION OF LONGSHORE COMPONENT OF ENERGY FLUX

The total energy of a water wave per unit length of wave crest may be expressed to a first approximation by:

$$E = \frac{\rho g H^2 L}{8} \qquad (1)$$

where ρ = density of water, g = acceleration of gravity, H = wave height, and L = wave length (U.S. Army Corps of Engineers, 1961). However, the total energy of a wave is not forward-moving energy. In deep water, approximately 1/2 the energy is due to the oscillatory movement of water particles (kinetic energy) and the remainder moves along with the wave form and is termed potential energy. As a wave approaches the breaker zone, the potential energy is essentially conserved and the kinetic energy decreases to zero as the wave reaches the point of breaking. The potential energy of a wave can be expressed by:

$$E_o = 1/2\ b_o\ E_{T_o} \quad \text{(deep water energy)} \qquad (2)$$

$$E = n\ b\ E_T \quad \text{(shallow water energy)} \qquad (3)$$

E_o represents deep water ($> 1/2\ L$) potential energy and E represents shallow water ($< 1/2\ L$) potential energy. The term n is a fraction varying from 1/2 to 1, determined by its transition from deep to shallow water. The subscript "o" always denotes deep-water conditions. The b_o and b terms are determined by wave refraction analysis (Munk and Traylor, 1947). "b_o" is the distance between two lines, called orthogonals, constructed perpendicular to a deep-water wave crest. As a wave crest moves into shore, it is refracted by bottom topography such that the distance between the orthogonals will have some new value "b". The refraction analysis is based on the assumption that

no energy flows laterally along a wave crest. Thus, the total amount of energy contained in a deep-water wave crest between two orthogonals (b_o) will be the same as the total energy contained between the final orthogonals (b) at some point near shore.

Assuming conservation of energy, we can equate the two expressions:

$$\frac{E_T}{E_{T_o}} = \left(\frac{1}{2}\right)\left(\frac{1}{n}\right)\left(\frac{b_o}{b}\right)$$

and, if the wave is shallow water, n = 1:

$$E_T = \frac{E_{T_o}}{2}\left(\frac{b_o}{b}\right) \qquad (4)$$

which represents the potential energy of a wave in shallow water.

Waves generally approach a coast at an angle. Refraction tends to cause wave crests to align themselves parallel to the shoreline, but is seldom completely successful. Thus, the wave crest, and its associated energy, reach the coast at some angle, α. Assuming no dissipation or reflection, the rate of transport of wave energy between adjacent orthogonals to a wave crest remains constant for temporally constant deep-water wave characteristics. This wave energy can be treated as a vector, and may be resolved into a longshore component and a component normal to the shore. The longshore component could then be a relative measure of the direction of sediment movement (Eagleson and Johnson, 1960). The following equation for longshore energy flux may be developed from the adjoining energy diagram.

$$E_{L.S.} = E_T \sin \alpha \cos \alpha \, dx$$

= longshore component of energy associated with a given length of shoreline

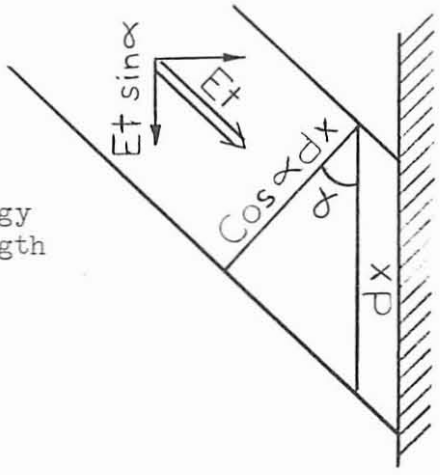

(5)

In order to determine the energy flux over a given time interval, the energy per wave may be multiplied by the number of waves occurring in the time interval. The number of waves may be determined by dividing the number of seconds in the time interval by the significant period (T_s) of the given set of wave statistics.

$$E_{L.S.}\left(\frac{t}{T_s}\right) = E_T\left(\frac{t}{T_s}\right) \sin \alpha \cos \alpha \, dx$$

$$= \frac{E_{T_o}}{2}\left(\frac{b_o}{b}\right)\left(\frac{t}{T_s}\right) \sin \alpha \cos \alpha \, dx \qquad (6)$$

Substituting the value for E_{T_o} from eq. (1), the form is obtained:

$$E_{L.S.} = \frac{\rho g H^2 L}{8}\left(\frac{b_o}{b}\right)\left(\frac{t}{T_s}\right) \sin \alpha \cos \alpha \, dx \qquad (7)$$

An expression involving the period (T) may be substituted for the wave length (L) in the above equation through a wave velocity equation for Stokes' waves in deep water.

$$C^2 = \frac{gL}{2\pi} \text{ and } C = \frac{L}{T}$$

thus

$$\frac{L^2}{T^2} = \frac{gL}{2\pi} \text{ and } L = \frac{gT^2}{2\pi}$$

Substituting the value for L into eq. (7) the final form is obtained.

$$E_{L.S.} = \left(\frac{\rho g^2}{2\pi}\right) H_o^2 \, T \left(\frac{b_o}{b}\right) t \sin \alpha \cos \alpha \, dx$$

$$= 20.5 \, H_o^2 \, T \left(\frac{b_o}{b}\right) t \sin \alpha \cos \alpha \, dx \qquad (8)$$

Energy in foot-pounds per foot of beach per time (day).

In order to determine the energy flux for a given value of H and T, multiply equation (8) by the percentage of time that the above value of wave height and period occur.

National Marine Consultants (1961b) have determined average sea and swell conditions for a point off the Columbia River. They have also constructed wave refraction diagrams (1961a) from which (b_o/b) values, and angle of approach may be determined. The above equation (8) may then be solved for average monthly and yearly longshore energy flux values (Table IX).

APPENDIX II

HEAVY MINERAL ANALYSIS

A heavy mineral analysis was made for samples that represent the full length of the study area using a modification of the frozen bromoform technique developed by R. A. MacKay (Fessenden, 1959). The procedure is outlined in the following steps:

1. Sediments of the 3.0 to 3.5 phi size range were selected for analysis. This is the smallest size range that can be easily handled and yet contain a reasonably high percentage of heavy minerals. The same size was used throughout for purposes of comparison.
2. Each sample was reduced to a 1-2 gram size using an Otto microsplitter, and placed in a centrifuge tube.
3. Bromoform (Sp. Gr. 2.85) was added to each sample and the mixture centrifuged for 10 minutes.
4. The lower portion of each centrifuge tube was placed in an acetone-dry ice mixture until the bromoform was frozen.
5. The unfrozen bromoform was decanted and filtered to remove the associated minerals. The minerals were dried, weighed, and termed "light minerals."
6. The frozen bromoform was allowed to melt and the procedure was repeated. The minerals obtained were termed "heavy minerals."
7. The percent heavy minerals by weight was determined for each sample (Table V).
8. A suite of fairly common heavy minerals was selected for determination of relative frequencies (Table VI).

APPENDIX III

MECHANICAL ANALYSIS

The procedure was modified from that of the Sediment Analysis Laboratory, Department of Oceanography, University of Washington. The modifications were permissible because all of the samples were of sand size, containing very little silt or clay sized particles.

1. Immediately after each sample was collected it was placed in a heavy plastic bag.
2. A representative portion of each sample was split off in the laboratory, placed in a tared 100-milliliter beaker and dried in an oven at 95°C to constant weight. It was then placed in a desiccator, cooled, and weighed to the nearest milligram.
3. Each sample was wet-sieved through a 4 phi (62 micron) sieve to remove most of the fine fraction. The fine fraction was retained for further treatment if necessary. The coarse fraction was again placed in a tared, 100-milliliter beaker, dried, and weighed.
4. Each sample was size graded according to the Wentworth (1922) scale using phi (ϕ) notation as described by Krumbein and Pettijohn (1938). The size in phi values is defined as the negative log to the base two of the diameter in millimeters (phi = $-\log_2$ size in millimeters).

   Coarse Fraction: The coarse fraction (< 4 phi or > 62 microns) was graded using sieves with a 0.5 phi unit progression. The sieves were shaken for 10 minutes in a Ro-tap

automatic shaking machine (W. S. Tyler Co., Cleveland, Ohio). The fraction retained on each sieve was weighed to the nearest milligram and stored in vials for future use.

Fine Fraction: The pan fraction (> 4.0 phi) obtained from the dry sieving was added to the fine fraction obtained by wet sieving. The total fine fraction weight was determined by adding the weight of the pan fraction to the difference in weights before and after wet sieving. This value should represent a maximum value for the fine fraction, as it includes any sediment loss due to the wet sieving process plus the weight of salt in the sample. Whenever the fine fraction amounted to 5 percent or more of the sample, a pipette analysis was performed to determine the size grades between 4 phi and 11 phi. Wadell's correction to Stokes' settling law was applied to determine the settling rates of the particles and their associated size grades (Krumbein and Pettijohn, 1938).

5. Statistics for describing the size distributions of each sample were obtained by use of an I.B.M. 709 computer (Creager, McManus, and Collias, 1962). Folk and Ward (1957) statistical parameters require that the measured sizes include the middle 90 percent of the total range of size distribution in a sample. For this reason the pipette analysis need not be carried out on the fine fraction when it constitutes less than 5 percent of the total sediment.

UNCLASSIFIED TECHNICAL REPORTS DISTRIBUTION LIST
for OCEANOGRAPHIC CONTRACTORS
of the GEOPHYSICS BRANCH
of the OFFICE OF NAVAL RESEARCH
(Revised October 1963)

DEPARTMENT OF DEFENSE

1 Director of Defense Research & Engineering
Attn: Coordinating Committee on Science
Pentagon
Washington 25, D. C.

1 Attn: Office, Assistant Director (Research)

NAVY

2 Office of Naval Research
Geophysics Branch (Code 416)
Washington 25, D. C.

Office of Naval Research
Washington 25, D. C.
1 Attn: Biology Branch (Code 446)
1 Attn: Surface Branch (Code 463)
1 Attn: Undersea Warfare (Code 466)
1 Attn: Special Projects (Code 418)

1 Commanding Officer
Office of Naval Research Branch
495 Summer Street
Boston 10, Massachusetts

1 Commanding Officer
Office of Naval Research Branch
207 West 24th Street
New York 11, New York

1 Commanding Officer
Office of Naval Research Branch
230 N. Michigan Avenue
Chicago, Illinois 60601

1 Commanding Officer
Office of Naval Research Branch
1000 Geary Street
San Francisco 9, California

1 Commanding Officer
Office of Naval Research Branch
1030 East Green Street
Pasadena 1, California

10 Commanding Officer
Office of Naval Research Branch
Navy #100, Fleet Post Office
New York, New York

1 Oceanographer
Office of Naval Research
Navy #100, Box 39
Fleet Post Office
New York, New York

1 Contract Administrator
Southeastern Area
Office of Naval Research
2110 "G" Street, N. W.
Washington 7, D. C.

1 ONR Special Representative
c/o Hudson Laboratories
Columbia University
145 Palisade Street
Dobbs Ferry, New York

6 Director
Naval Research Laboratory
Attn: Code 5500
Washington 25, D. C.

(Note: 3 copies are forwarded by the above addressee to the British Joint Services Staff for further distribution in England and Canada.)

1 Oceanographer
Chief of Naval Operations
OP-09B5
Washington 25, D. C.

1 Commander
U. S. Naval Oceanographic Office
Washington 25, D. C.
Attn: Library (Code 1640)

1 U. S. Naval Branch
Oceanographic Office
Navy 3923, Box 77, F.P.O.
San Francisco, California

Chief, Bureau of Naval Weapons
Department of the Navy
Washington 25, D. C.
1 Attn: FASS
1 Attn: RU-222

1 Office of the U. S. Naval
Weather Service
U. S. Naval Station
Washington 25, D. C.

1 Chief, Bureau of Yards & Docks
Office of Research
Department of the Navy
Washington 25, D. C.
Attn: Code 70

1 Commanding Officer & Director
U. S. Navy Electronics Laboratory
San Diego 52, California
1 Attn: Code 2201
1 Attn: Code 2420

1 Commanding Officer & Director
U. S. Naval Civil Engineering
Laboratory
Port Hueneme, California
Attn: Code L54

1 Code 3145
Box 7
Pt. Mugu Missile Range
Pt. Mugu, California

1 Commander, Naval Ordnance Laboratory
White Oak, Silver Spring, Maryland
Attn: E. Liberman, Librarian

1 Commanding Officer
Naval Ordnance Test Station
China Lake, California
1 Attn: Code 753
1 Attn: Code 508

1 Commanding Officer
Naval Radiological Defense Laboratory
San Francisco, California

1 Commanding Officer
U. S. Naval Underwater Ordnance
Station
Newport, Rhode Island

Chief, Bureau of Ships
Department of the Navy
Washington 25, D. C.
1 Attn: Code 373

1 Officer-in-Charge
U. S. Navy Weather Research
Facility
Naval Air Station, Bldg. R-48
Norfolk, Virginia

1 U. S. Fleet Weather Facility
U. S. Naval Station
San Diego 35, California

1 Commanding Officer
U. S. Navy Air Development
Center
Johnsville, Pennsylvania
Attn: NADC Library

1 Superintendent
U. S. Naval Academy
Annapolis, Maryland

2 Department of Meteorology &
Oceanography
U. S. Naval Postgraduate School
Monterey, California

1 Commanding Officer
U. S. Naval Underwater Sound
Laboratory
New London, Connecticut

1 Commanding Officer
U. S. Navy Mine Defense Lab.
Panama City, Florida

1 Commanding Officer
U. S. Fleet Weather Central
Navy Department
Washington 25, D. C.

1 Officer-in-Charge
U. S. Fleet Numerical Weather
Facility
Monterey, California

AIR FORCE

1 Hdqtrs., Air Weather Service
(AWSS/TIPD)
U. S. Air Force
Scott Air Force Base, Illinois

1 ARCRL (CRZF)
L. G. Hanscom Field
Bedford, Massachusetts

ARMY

1 Army Research Office
Office of the Chief of R & D
Department of the Army
Washington 25, D. C.

1 U. S. Army Beach Erosion Board
5201 Little Falls Road, N. W.
Washington 16, D. C.

1 Army Research Office
Washington 25, D. C.
Attn: Environmental Sciences Div.

OTHER U. S. GOVERNMENT AGENCIES

1 Office of Technical Services
Department of Commerce
Washington 25, D. C.

20 Defense Documentation Center
Cameron Station
Alexandria, Virginia

2 National Research Council
2101 Constitution Avenue
Washington 25, D. C.
Attn: Committee on Undersea Warfare
Attn: Committee on Oceanography

1 Laboratory Director
Biological Laboratory
Bureau of Commercial Fisheries
P. O. Box 6121, Pt. Loma Street
San Diego, California

1 Commandant (OSR-2)
U. S. Coast Guard
Washington 25, D. C.

1 Commanding Officer
Coast Guard Oceanographic Unit
Bldg. 159, Navy Yard Annex
Washington 25, D. C.

1 Director
Coast & Geodetic Survey
U. S. Department of Commerce
Washington 25, D. C.
Attn: Office of Oceanography

1 Geological Division
Marine Geology Unit
U. S. Geological Survey
Washington 25, D. C.

1 Director of Meteorological Research
U. S. Weather Bureau
Washington 25, D. C.

1 Director
U. S. Army Engineers Waterways
Experiment Station
Vicksburg, Mississippi
Attn: Research Center Library

1 Laboratory Director
Bureau of Commercial Fisheries
Biological Laboratory
450-B Jordan Hall
Stanford, California

1 Bureau of Commercial Fisheries
U. S. Fish & Wildlife Service
Post Office Box 3830
Honolulu 12, Hawaii
1 Attn: Librarian

1 Laboratory Director
Biological Laboratory
Bureau of Commercial Fisheries
P. O. Box 3098, Fort Crockett
Galveston, Texas

1 Laboratory Director
Biological Laboratory, Auke Bay
Bureau of Commercial Fisheries
P. O. Box 1155
Juneau, Alaska

1 Laboratory Director
Biological Laboratory
Bureau of Commercial Fisheries
P. O. Box 6
Woods Hole, Massachusetts

1 Laboratory Director
Biological Laboratory
Bureau of Commercial Fisheries
P. O. Box 280
Brunswick, Georgia

1 Laboratory Director
Biological Laboratory
Bureau of Commercial Fisheries
P. O. Box 271
La Jolla, California

1 Bureau of Sport Fisheries & Wildlife
U. S. Fish and Wildlife Service
Sandy Hook Marine Laboratory
P. O. Box 428
Highlands, New Jersey
Attn: Librarian

1 Director
National Oceanographic Data Center
Washington 25, D. C.

2 Defense Research Member
Canadian Joint Staff
2450 Massachusetts Avenue, N. W.
Washington 8, D. C.

2 Library, U. S. Weather Bureau
Washington 25, D. C.

1 Director, Biological Laboratory
Bureau of Commercial Fisheries
Navy Yard Annex
Building 74
Washington 25, D. C.

2 Director, Bureau of Commercial Fisheries
U. S. Fish & Wildlife Service
Department of Interior
Washington 25, D. C.

1 Dr. Orlo E. Childs
U. S. Geological Survey
345 Middlefield Road
Menlo Park, California

1 Dr. John S. Schlee
U. S. Geological Survey
c/o Woods Hole Oceanographic Institution
Woods Hole, Massachusetts

RESEARCH LABORATORIES

2 Director
Woods Hole Oceanographic Inst.
Woods Hole, Massachusetts

3 Project Officer
Laboratory of Oceanography
Woods Hole, Massachusetts

1 Director
Narragansett Marine Laboratory
University of Rhode Island
Kingston, Rhode Island

1 Bingham Oceanographic Labs.
Yale University
New Haven, Connecticut

1 Gulf Coast Research Laboratory
Post Office Box
Ocean Springs, Mississippi
Attn: Librarian

1 Chairman, Department of Meteorology and Oceanography
New York University
New York 53, New York

1 Director
Lamont Geological Observatory
Torrey Cliff
Palisades, New York

1 Director
Hudson Laboratories
145 Palisade Street
Dobbs Ferry, New York

1 Great Lakes Research Division
Institute of Science & Technology
University of Michigan
Ann Arbor, Michigan
1 Attn: Dr. John C. Ayers

1 Dr. Harold Haskins
Rutgers University
New Brunswick, New Jersey

1 Director
Chesapeake Bay Institute
Johns Hopkins University
121 Maryland Hall
Baltimore 18, Maryland

1 Mail No. J-3009
The Martin Company
Baltimore 3, Maryland
Attn: J. D. Pierson

1 Mr. Henry D. Simmons, Chief
Estuaries Section
Waterways Experiment Station
Corps of Engineers
Vicksburg, Mississippi

1 Director, Marine Laboratory
University of Miami
#1 Rickenbacker Causeway
Virginia Key
Miami 49, Florida

1 Nestor C. L. Granelli
Department of Geology
Columbia University
Palisades, New York

2 Head, Department of Oceanography
& Meteorology
Texas A & M College
College Station, Texas

1 Director
Scripps Institution of Oceanography
La Jolla, California

1 Allan Hancock Foundation
University Park
Los Angeles 7, California

1 Head, Department of Oceanography
Oregon State University
Corvallis, Oregon

1 Department of Engineering
University of California
Berkeley, California

1 Director
Arctic Research Laboratory
Barrow, Alaska

1 Dr. C. I. Beard
Boeing Scientific Research Labs.
P. O. Box 3981
Seattle 24, Washington

1 Head, Department of Oceanography
University of Washington
Seattle 5, Washington

1 Geophysical Institute of the
University of Alaska
College, Alaska

1 Director
Bermuda Biological Station
for Research
St. Georges, Bermuda

1 Technical Information Center, CU-201
Lockheed Missile and Space Division
3251 Hanover Street
Palo Alto, California

1 University of Pittsburgh
Environmental Sanitation
Department of Public Health Practice
Graduate School of Public Health
Pittsburgh 13, Pennsylvania

1 Director
Hawaiian Marine Laboratory
University of Hawaii
Honolulu, Hawaii

1 Dr. F. B. Berger
General Precision Laboratory
Pleasantville, New York

1 Dr. J. A. Gast
Wildlife Building
Humboldt State College
Arcata, California

1 Department of Geodesy & Geophysics
Cambridge University
Cambridge, England

1 Applied Physics Laboratory
University of Washington
1013 NE Fortieth Street
Seattle 5, Washington

1 Documents Division - ml
University of Illinois Library
Urbana, Illinois

1 Director
Ocean Research Institute
University of Tokyo
Tokyo, Japan

1 Marine Biological Association
of the United Kingdom
The Laboratory
Citadel Hill
Plymouth, England

1 ASW Information Research Unit
Building 80, Plant A-1
Lockheed-California Company
Burbank, California

1 New Zealand Oceanographic Institute
Department of Scientific and
Industrial Research
P. O. Box 8009
Wellington, New Zealand
Attn: Librarian

1 President
Osservatorio Geofisico Sperimentale
Trieste, Italy

1 Advanced Research Projects Agency
Attn: Nuclear Test Detection Office
The Pentagon
Washington 25, D. C.

1 Chemistry Department
College of Engineering
University of Wisconsin
Madison 6, Wisconsin

1 American Biophysical Research Lab.
P. O. Box 552
Lansdale, Pennsylvania

1 Department of Geology & Geophysics
Massachusetts Institute of Technology
Cambridge 39, Massachusetts

1 Institute of Geophysics
University of Hawaii
Honolulu 14, Hawaii

1 Dr. Wilbur Marks
Oceanics, Inc.
114 East 40th Street
New York 16, New York

1 Mr. Neil L. Brown
Bissett-Berman Corporation
"G" Street Pier
San Diego, California